A Geometric Characterization of Observability in Inertial Parameter Identification

Patrick M. Wensing, Günter Niemeyer, Jean-Jacques E. Slotine

***Abstract*—This paper presents an algorithm to geometrically characterize the identifiability of inertial parameters in system identification of an articulated robot. The algorithm can be applied to general open-chain kinematic trees ranging from industrial manipulators to legged robots, and it is the first solution for this broad set of systems that is provably correct. The high-level operation of the algorithm is based on a key observation: Undetectable changes in inertial parameters can be represented as sequences of inertial transfers across the joints. Drawing on the exponential parameterization of rigid-body kinematics, undetectable inertial transfers are analyzed in terms of observability from linear systems theory. This analysis can be applied recursively, and lends an overall complexity of $O(N)$ to characterize parameter identifiability for a system of N bodies. MATLAB source code for the new algorithm is provided.**

I. Introduction

A classic problem in robotics is the identification of inertial parameters (mass, center of mass, and inertia) for each link of a mechanism. This problem has received attention through multiple decades, with original work on identification of manipulators [1]–[3] seeing extensions to identification of mobile robots and humans in more recent applications [4]–[9]. Across domains, an enabling property is that the inverse dynamics of a rigid-body system are linear in its inertial parameters, motivating the use of least-squares solutions to identify parameters from the measurement of joint kinematics, joint torques, and external forces.

It is well known, however, that not all inertial parameters are identifiable from these measurements [1]. This observation has motivated studying which parameters (or combinations thereof) can theoretically be identified from an infinite amount of data [2], [6], [10]–[15]. This problem is one of characterizing the *structural identifiability* [16] of a model, and it is emphasized that this problem is distinct from that of fitting a model to experimental data. Naturally, the accuracy of any identified model depends both on the accuracy of the model form assumed and the accuracy of the data collected. Addressing how uncertainty in measurements relates to uncertainty in identified parameters (e.g., [17], [18]) is, by contract, a problem of characterizing *practical identifiability*. In short, structural identifiability considers what model properties can be identified from ideal data, whereas practical identifiability considers how non-ideal data impacts the inferred model.

This paper presents new tools for characterizing the structural identifiability of a rigid-body system by drawing upon geometric characterizations of the problem. We provide an algorithm that takes a kinematic model as an input, and returns the linear combinations of the system's inertial parameters that are identifiable from measurements of the joint kinematics, joint torques, and external forces. The approach taken offers an alternative to previous numerical (e.g., [19]) or symbolic approaches (e.g., [10], [20]) to the problem. The main benefit of our approach is that the algorithm comes with a theoretical proof of correctness that holds for arbitrary open-chain fixed- or floating-base systems with generic joint types. This proof of correctness is achieved by working with spatial inertias in a parameterization-free sense and only adopting inertial parameters for implementation of the theory.

We show that undetectable changes in the spatial inertias of the links can be represented by exchanges of mass and inertia between neighboring bodies. Exchanges are considered undetectable if they leave the system dynamics unchanged across the entire state space. Addressing this infinity of possibilities is the main hurdle that has previously prevented a rigorous treatment of structural identifiability for general robot systems.

A. Related previous work

In the early work on system identification, a great deal of emphasis was placed on determining minimal sets of parameters (base parameters) to be identified [19]. Base parameters group together linear combinations of link parameters that always show up together in the equations of motion. Isolating these groupings enables the use of a reduced set of parameters within symbolic expressions and likewise can be used to accelerate dynamics computations [22], such as the Recursive-Newton-Euler Algorithm (RNEA). The use of a minimal set of base parameters also enables least-squares identification problems [1] to have a unique solution.

Since this work back in the 1980s and 90s, increases in computing power and new identification methodologies suggest revisiting these original motivations. Regarding computation power, RNEA can now be carried out in microseconds for complex systems without needing to reduce the parameter set [23]. In terms of methodology, recent advances in enforcing physical consistency of the parameters [7], [24], [25] and geometric regularization [9], [26] jointly suggest the benefits of considering the full parameter set when carrying out identification.

Despite these recent advances, structural identifiability considerations remain fundamental for robot system identification. Recall that structural identifiability analysis characterizes which parameters (or combinations) can be deduced from an *infinite* amount of training data. Methods that design exciting trajectories [3], [27]–[29] seek to maximally identify model information with a *finite* amount of training data. It

	Type	General Joints	Fixed Base.	Floating Base	Closed Chains	Provably Correct
Ayusawa *et al.*, 2014 [6]	Symbolic	✓		✓		✓
Gautier *et al.*, 1990 [10]	Symbolic		✓			
Gautier *et al.*, 1991 [19]	Numeric	✓	✓	✓	✓	
Ros *et al.*, 2015 [21]	Symbolic		✓		✓	
This Paper	**Geometric**	✓	✓	✓	Rotors Only	✓

TABLE I
FEATURE COMPARISON.

is only possible to certify that a given dataset is maximally exciting, however, via comparison to a structural identifiability analysis. Another motivation for characterizing base parameters comes from instrumental variable identification techniques [30]–[32] that address model bias from noisy data, but currently require the use of a non-redundant model parameterizaiton. Methods that characterize uncertainty in the parameter estimates likewise only do so through considering uncertainty in the base parameters [17], [18]. Additionally, floating-base systems are often identified in restricted setups (e.g., with the base fixed [25], [33], [34]) and so it is important to understand how these setups affect model identifiability.

Previous methods for characterizing identifiability can be grouped into symbolic and numerical approaches. Symbolic approaches originally proceeded by considering common groupings of parameters that appear within the equations of motion [20], [35], [36]. This strategy can become untenable at a system-level scale due to the complexity of the equations of motion. Thus, other work focused on carrying out regroupings of parameters by hand for special cases such as revolute manipulators with parallel or perpendicular joints [10], [11], [13]. Despite these restrictions, many special cases have to be considered, for example, whether joints are revolute or prismatic, parallel or orthogonal to each other, parallel or orthogonal to gravity, and combinations of the above. Each time that a new symbolic grouping is isolated, it reduces the upper bound on the number of identifiable parameters of the model. If all groupings are discovered, then the identifiability of the model is correctly characterized. Yet, if regroupings are missed, it leads one to believe that more parameters are identifiable than actually are. The complexity of the many cases to be considered makes arriving at the correct result a non-trivial task. By comparison, the method herein does not require any special cases, and characterizes identifiability through a unified geometric treatment.

On the flip side, numerical methods for assessing identifiability (e.g., [19]) provide a lower bound on the number of identifiable parameters of the model. Methods in this class often generate a finite set of random data which is assumed to be maximally exciting. If the data is indeed maximally exciting, and there are no numerical issues, then correct conclusions can be drawn regarding the identifiability of the model. In cases when the data is not maximally exciting, the number of identifiable parameters is underestimated. Thus, such methods generally provide a lower bound on the number of identifiable parameters, while symbolic methods provide an upper bound. By combining these together [19] the correctness of both can be checked. Overall, neither the symbolic or numeric approaches individually are provably correct for general mechanisms.

A complementary approach to considering parameter regroupings is to consider undetectable transfers of inertia between pairs of bodies across each joint. This strategy was developed originally in [37] for use with floating-base systems with revolute and prismatic joints. It was later independently discovered by Chen and collegaues for 2D [14] and 3D [38] mechanisms, and developed further by Ros et al. [15], [21], [39]. These latter papers represent the state of the art in base parameter determination. However, much like original symbolic approaches (e.g., [10]) they require a skilled individual to exercise discretion in applying a set of special rules for determining identifiable parameters of links with motion restrictions close to the ground. By comparison, our algorithm is fully automatic. The user provides a model description (e.g., specifying the kinematic data found in a URDF file), and our algorithm provides provably correct description of which parameter combinations are identifiable, and which are not.

B. Contribution

The main contribution of this paper is the first provably correct algorithm to characterize the identifiable inertial parameter combinations for general fixed- and floating-base open-chain systems (Tab. I). The algorithm is named the Recursive-Parameter-Nullspace Algorithm (RPNA) and has a structure reminiscent of the outward kinematics pass of the RNEA. Rather than computing the velocities of each link on the outward pass, we geometrically characterize all possible velocities of each link. This information enables the algorithm to automatically detect motion restrictions for each body and to assess how those restrictions influence parameter identifiability. More specifically, by drawing upon the exponential characterization of kinematics, the approach employs controllability analysis from linear systems theory to characterize possible motions experienced by each link. It then uses observability analysis to determine exchanges of mass and inertia between pairs of bodies that can be carried out without impact on the system dynamics. Chaining these results recursively allows us to provably describe the identifiable parameter combinations for the system as a whole.

Our theoretical development proceeds parameterization-free while employing inertial parameters only in implementation. Correspondingly, as a minor contribution, we provide an updated treatment of identifiability employing tools from spatial vector algebra [40], which can be readily translated to

Lie group/algebra notation. We hope that this more modern treatment will be an asset to the reader toward more rapidly interpreting previous strategies (e.g., [11], [19], etc.) that focused on detailed symbolic expressions.

C. Organization

The paper is organized as follows. Section II introduces the main concepts of the paper at a high level. Concepts are demonstrated considering inertia transfers between two rigid bodies connected by a single joint. We consider separately the cases when the bodies can experience general spatial motions (Sec. III) vs. having motion restrictions (Sec. IV). These developments then serve as the main building blocks for a recursive treatment of identifiability in chains of bodies (Sec. V). Section VI provides description of the RPNA. Extensions of the basic algorithm to kinematics trees, multi-DoF joints, and simple closed-chain systems are provided in Section VII. Results in Section VIII consider system-level identifiability for classical manipulators, the PUMA & SCARA, as well as a mobile robot, the Cheetah 3. As a key practical takeaway, we illustrate the pitfalls of constrained identification experiments that have often been used to identify individual limbs of mobile legged systems. Concluding comments are provided in Section IX.

II. Main Concepts

We consider identifying a rigid-body robot with N bodies whose joint-space dynamics take the standard form

$$\mathbf{H}(\mathbf{q})\,\ddot{\mathbf{q}} + \mathbf{c}(\mathbf{q},\dot{\mathbf{q}}) + \mathbf{g}(\mathbf{q}) = \boldsymbol{\tau} \tag{1}$$

with $\mathbf{q}$ the configuration variable, $\mathbf{H}$ the mass matrix, $\mathbf{c}$ and $\mathbf{g}$ the Coriolis and gravity forces, and $\boldsymbol{\tau}$ the generalized force. For a fixed-base system, $\boldsymbol{\tau}$ represents a vector of joint torques. For a floating-base system in contact, we partition $\dot{\mathbf{q}} = [\dot{\mathbf{q}}_B^\top\ \dot{\mathbf{q}}_J^\top]^\top$ where $\dot{\mathbf{q}}_B \in \mathbb{R}^6$ characterizes the linear and angular velocity of the base, and $\dot{\mathbf{q}}_J$ the joint velocities. In that case, the generalized force takes the form:

$$\boldsymbol{\tau} = \begin{bmatrix}\mathbf{0}_{6\times 1}\\ \boldsymbol{\tau}_J\end{bmatrix} + \mathbf{J}(\mathbf{q})^\top \mathbf{f} \tag{2}$$

where $\boldsymbol{\tau}_J$ are the joint torques, $\mathbf{J}$ the Jacobian for the contacts, and $\mathbf{f}$ the contact forces.

In either case, it is well known that (1) can be expressed linearly in the inertial parameters $\boldsymbol{\pi} \in \mathbb{R}^{10N}$ of the bodies, which include masses, first moments, and rotational inertias:

$$\boldsymbol{\tau} = \mathbf{Y}(\mathbf{q},\dot{\mathbf{q}},\ddot{\mathbf{q}})\,\boldsymbol{\pi} \tag{3}$$

where $\mathbf{Y}$ is the classical regressor [1]. Unidentifiable parameters of the system are formally given by the intersection of an infinite number of nullspaces

$$\mathcal{N} = \{\delta\boldsymbol{\pi} \in \mathbb{R}^{10N} \mid \mathbf{Y}(\mathbf{q},\dot{\mathbf{q}},\ddot{\mathbf{q}})\,\delta\boldsymbol{\pi} = \mathbf{0},\ \forall\, \mathbf{q},\dot{\mathbf{q}},\ddot{\mathbf{q}}\}$$

For any $\delta\boldsymbol{\pi} \in \mathcal{N}$, we say that the change $\delta\boldsymbol{\pi}$ does not affect the dynamics, or equivalently that it is not identifiable through measurement of the generalized force $\boldsymbol{\tau}$. For a fixed-base system, this statement is the same as saying that $\delta\boldsymbol{\pi}$ is undetectable from measurement of the joint torques. For a floating-base system, it is equivalent to $\delta\boldsymbol{\pi}$ being undetectable from measurement of the joint torques and external forces.

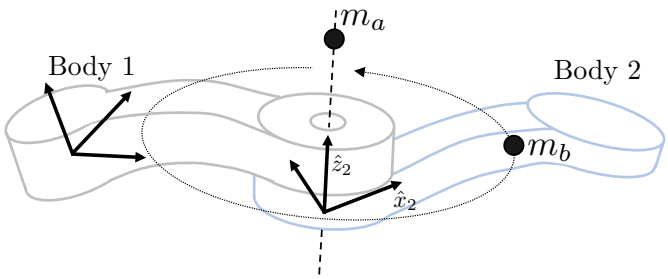

Fig. 1. Masses m_a and m_b are rigidly attached to body 2. The inertial properties of mass m_a are felt by body 1 in a fixed way with changes in angle of the connecting joint, while the inertial properties of mass m_b are felt in a variable way.

Note that the set $\mathcal{N}$ is a linear subspace, and any basis for it will generally consist of combinations of parameters from multiple bodies. In deriving a basis for $\mathcal{N}$, we will show that it is enough to consider combinations of parameters from only two neighboring bodies at a time, and that these combinations represent an inertia transfer between the bodies.

Toward arriving at this result, we consider parameters of a body as being identified via one of two mechanisms: (1) directly via the torque on the preceding joint, or (2) indirectly via joint torques earlier in the kinematic chain. We note that in terms of the total inertia felt earlier in the chain, the inertia of a body combines with its parent, and that this total inertia depends on the joint configuration. Thus, this second mechanism relies on variations in how the inertia of a body is viewed by its parent as the joint moves. Intuitively, if a child parameter adds with the parent inertia in a fixed manner, then the parent will be unable to distinguish this parameter from its own. In this case, the child parameter may only be identifiable in combination with the parent parameters. In contrast, if a child parameter adds with the parent inertia in a variable manner, then these variations can be used to identify the parameter through indirect means via joint torques downstream. Figure 1 illustrates this idea at a high level, showing two masses attached to body 2. The inertial properties of mass m_a are felt on the predecessor in a fixed manner with changes in joint angle. In contrast, the inertial properties of mass m_b are felt by body 1 in a variable way with joint angle.

Inverting these two mechanisms, a parameter contributes to the dimension of $\mathcal{N}$ if (1) it cannot be sensed via the preceding joint torque and (2) it adds to the parent inertia in a fixed way despite changes in joint angle. In this case, numeric values for the parameter can be assigned to the parent or the child without affect on the overall dynamics. For instance, the inertial properties from mass m_a in Fig. 1 satisfy both these conditions, and thus mass m_a could be assigned to either body without affecting the system dynamics. This freedom to exchange m_a between bodies captures the conceptual idea of an inertial transfer across the joint. The combination of all such undetectable exchanges will be shown to span $\mathcal{N}$.

To analyze the parameter combinations that have no effect on the system dynamics, we will equivalently consider param-

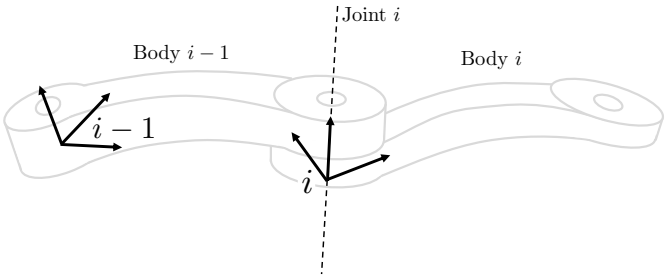

Fig. 2. Example two-body floating-base system. Body i-1 can move freely body i is attached via a single-degree-of-freedom joint (revolute as shown). Frames i-1 and i-1 are rigidly attached to bodies i-1 and i respectively. The frames coincide in the case when the joint angle q satisfies $q = 0$.

eter changes that do not modify the kinetic or gravitational potential energy[1]. To begin, focus will be placed on the kinetic energy, as simple modifications to our main developments allow the effects of gravity to be addressed. Effects of rotational and linear kinetic energy will be captured together using 6D spatial notation [40]. For example, the kinetic energy of a single body takes the form

$$T = \frac{1}{2}\mathbf{v}^\top \mathbf{I}\mathbf{v}$$

with $\mathbf{v} \in \mathbb{R}^6$ its spatial velocity and $\mathbf{I} \in \mathbb{R}^{6\times 6}$ its spatial inertia. These spatial quantities are given by

$$\mathbf{v} = \begin{bmatrix} \omega_x \\ \omega_y \\ \omega_z \\ v_x \\ v_y \\ v_z \end{bmatrix} \qquad \mathbf{I} = \begin{bmatrix} I_{xx} & I_{xy} & I_{xz} & 0 & -mc_z & mc_y \\ I_{xy} & I_{yy} & I_{yz} & mc_z & 0 & -mc_x \\ I_{xz} & I_{yz} & I_{zz} & -mc_y & mc_x & 0 \\ 0 & mc_z & -mc_y & m & 0 & 0 \\ -mc_z & 0 & mc_x & 0 & m & 0 \\ mc_y & -mc_x & 0 & 0 & 0 & m \end{bmatrix}$$

where $[\omega_x, \omega_y, \omega_z]^\top$ is the angular velocity of a body-fixed coordinate system, $[v_x, v_y, v_z]^\top$ the linear velocity of the origin of that system, m the body mass, $[c_x, c_y, c_z]^\top$ the CoM location in body coordinates, and I_{xx}, I_{yy}, etc. the mass moments and products of inertia about the body coordinate origin. The first moments are abbreviated as $h_x = mc_x$ for the x-axis and similarly for the others. Appendix A provides a review of spatial notation, with detailed background in [40].

Our preliminary analysis will consider the special case of rigid-body chains with bodies connected by single degree of freedom joints. Bodies are numbered 1 to N from the base to the end of the chain with a frame attached to each body (Fig. 2). Joint i connects body $i-1$ to body i, with its noted by $q_i \in \mathbb{R}$. Under these definitions, the spatial velocities of neighboring bodies are related as:

$$\mathbf{v}_i = {}^i\mathbf{X}_{i\text{-}1}(q_i)\,\mathbf{v}_{i\text{-}1} + \mathbf{\Phi}_i\,\dot{q}_i \tag{4}$$

where ${}^i\mathbf{X}_{i\text{-}1} \in \mathbb{R}^{6\times 6}$ is a spatial transform between frames and the vector $\mathbf{\Phi}_i \in \mathbb{R}^{6\times 1}$ describes the free motion for the joint. For instance, for a revolute joint about $\hat{z}_i$, $\mathbf{\Phi}_i = [0\,0\,1\,0\,0\,0]^\top$.

III. Two Body Case: General Spatial Motion

We begin by considering a single pair of bodies within the chain and using this simple case to mathematically develop the main ideas of the previous section. Consider bodies i-1 and i where body i-1 is able to move with any general spatial velocity. This case could occur, for example, if body i-1 were a floating base or if it were a body in a fixed base system that was far enough away from the base of the mechanism to experience all 6 spatial degrees of freedom in its movement.

A. Undetectable Changes in Inertia

We proceed to examine conditions under which the inertial parameters of these bodies can be changed without affecting the system's dynamics. To do so, we consider a collection of changes in inertias $\delta\mathbf{I}_{i\text{-}1}$ and $\delta\mathbf{I}_i$. For these changes to have no effect on the dynamics, they must not change the kinetic energy

$$\delta T = \frac{1}{2}\mathbf{v}_{i\text{-}1}^\top\,\delta\mathbf{I}_{i\text{-}1}\,\mathbf{v}_{i\text{-}1} + \frac{1}{2}\mathbf{v}_i^\top\,\delta\mathbf{I}_i\,\mathbf{v}_i = 0$$

Using (4), the variation δT can be factored as:

$$\frac{1}{2}\begin{bmatrix}\mathbf{v}_{i\text{-}1}\\ \dot{q}_i\end{bmatrix}^\top \begin{bmatrix} \delta\mathbf{I}_{i\text{-}1} + {}^i\mathbf{X}_{i\text{-}1}^\top\,\delta\mathbf{I}_i\,{}^i\mathbf{X}_{i\text{-}1} & {}^i\mathbf{X}_{i\text{-}1}^\top\,\delta\mathbf{I}_i\,\mathbf{\Phi}_i \\ \mathbf{\Phi}_i^\top\,\delta\mathbf{I}_i\,{}^i\mathbf{X}_{i\text{-}1} & \mathbf{\Phi}_i^\top\,\delta\mathbf{I}_i\,\mathbf{\Phi}_i \end{bmatrix} \begin{bmatrix}\mathbf{v}_{i\text{-}1}\\ \dot{q}_i\end{bmatrix}$$

For the kinetic energy variation δT to always be zero, each entry of the above matrix must be zero. Considering the off-diagonal blocks, this condition requires

$$0 = \mathbf{\Phi}_i^\top\,\delta\mathbf{I}_i \tag{5}$$

since ${}^i\mathbf{X}_{i\text{-}1}$ is full rank. The condition $\mathbf{\Phi}^\top\delta\mathbf{I}_i\mathbf{\Phi} = 0$ for the lower-right block is redundant with (5). For the upper-left block to be zero, it must be that

$$0 = \delta\mathbf{I}_{i\text{-}1} + {}^i\mathbf{X}_{i\text{-}1}^\top(q_i)\,\delta\mathbf{I}_i\,{}^i\mathbf{X}_{i\text{-}1}(q_i) \qquad \forall q_i \tag{6}$$

Toward more general results later the manuscript, we note that since $\mathbf{v}_{i\text{-}1}$ and $\mathbf{v}_i$ can individually take any values, these two conditions are equivalent to:

$$0 = \mathbf{\Phi}^\top\delta\mathbf{I}_i\mathbf{v}_i \qquad \forall\,\mathbf{v}_i \tag{7}$$

$$0 = \mathbf{v}_{i\text{-}1}^\top\left[\delta\mathbf{I}_{i\text{-}1} + {}^i\mathbf{X}_{i\text{-}1}^\top(q_i)\,\delta\mathbf{I}_i\,{}^i\mathbf{X}_{i\text{-}1}(q_i)\right]\mathbf{v}_{i\text{-}1} \qquad \forall \mathbf{v}_{i\text{-}1}, q_i \tag{8}$$

The first condition (7) encodes that changes in inertia $\delta\mathbf{I}_i$ must not change the projection of body's i momentum ($\mathbf{I}_i\mathbf{v}_i$) along the joint free mode $\mathbf{\Phi}_i$. For example, for a revolute joint about $\hat{z}_i$, the angular momentum about $\hat{z}_i$ must not change.

Returning to condition (6), we see the first appearance of a condition regarding an inertia transfer. The sum $\delta\mathbf{I}_{i\text{-}1} + {}^i\mathbf{X}_{i\text{-}1}^\top(q_i)\,\delta\mathbf{I}_i\,{}^i\mathbf{X}_{i\text{-}1}(q_i)$ represents the change in the total inertia of the two bodies combined. As a result, (6) requires that the combination of $\delta\mathbf{I}_{i\text{-}1}$ and $\delta\mathbf{I}_i$ must represent an even exchange of inertia between the bodies for all joint angles. In the case when when $q = 0$, (6) requires

$$\delta\mathbf{I}_{i\text{-}1} = -{}^i\mathbf{X}_{i\text{-}1}^\top(0)\,\delta\mathbf{I}_i\,{}^i\mathbf{X}_{i\text{-}1}(0) \qquad \text{(Transfer)} \tag{9}$$

which encodes an assignment for a transfer of inertia between the bodies. Considering changes in configuration via a time derivative of (6) then requires

$$\mathbf{0} = \frac{\mathrm{d}}{\mathrm{d}t}\left(-{}^i\mathbf{X}_{i\text{-}1}^\top(q_i)\,\delta\mathbf{I}_i\,{}^i\mathbf{X}_{i\text{-}1}(q_i)\right) \tag{10}$$

[1]More precisely, we will consider parameter variations that do not modify the rate of change in gravitational potential energy.

which enforces that the mapping of $\delta\mathbf{I}_i$ to body i-1 must not change over time. Consider the property [40, Eq. (2.45)]

$$\frac{\mathrm{d}}{\mathrm{d}t}{}^{i}\mathbf{X}_{i\text{-}1}(q_i) = -(\mathbf{\Phi}_i\dot{q}_i) \times {}^{i}\mathbf{X}_{i\text{-}1}(q_i)$$

where $(\mathbf{v})\times \in \mathbb{R}^{6\times 6}$ gives the spatial cross product matrix with its form noted further in Appendix A. This condition is simplified to:

$$\mathbf{0} = {}^{i}\mathbf{X}_{i\text{-}1}^{\top}\left[\,(\mathbf{\Phi}_i\dot{q}_i\times)^{\top}\delta\mathbf{I}_i + \delta\mathbf{I}_i(\mathbf{\Phi}_i\dot{q}_i\times)\,\right]{}^{i}\mathbf{X}_{i\text{-}1} \tag{11}$$

Since ${}^{i}\mathbf{X}_{i\text{-}1}$ is full rank and $\dot{q}_i$ can be chosen arbitrarily, (11) is equivalent to

$$(\mathbf{\Phi}_i\times)^{\top}\,\delta\mathbf{I}_i + \delta\mathbf{I}_i\,(\mathbf{\Phi}_i\times) = \mathbf{0} \tag{12}$$

To summarize, for two bodies that can experience general spatial motions, the exchange of inertias (9) not affecting the dynamics are those that 1) does not modify the projection of the second body's momentum along the joint and 2) is invariant to changes in configuration of the joint

$$\boxed{\begin{aligned}\mathbf{0} &= \mathbf{\Phi}_i^{\top}\delta\mathbf{I}_i && \text{(Momentum)} && (13)\\ \mathbf{0} &= (\mathbf{\Phi}_i\times)^{\top}\,\delta\mathbf{I}_i + \delta\mathbf{I}_i\,(\mathbf{\Phi}_i\times) && \text{(Invariance)} && (14)\end{aligned}}$$

We name these conditions the momentum, and invariance conditions. Conditions (13) and (14) are equivalent to [37, Eqs. (4.13) and (4.14)] and to [6, Eq. (41)]. Returning to the high-level description for how parameters are identified, the momentum condition (13) enforces that the changes $\delta\mathbf{I}_i$ must not affect local joint torque, where the invariance condition (14) enforces that the changes $\delta\mathbf{I}_i$ must not be detectable via how they are mapped to the parent.

B. Example: Revolute Joint

This subsection considers the conditions from the previous section in the case of a revolute connecting joint. We only consider parameter changes to body i, since the corresponding changes to body i-1 are determined with the transfer condition (9). Consider a revolute joint under the Denavit-Hartenberg convention $\mathbf{\Phi}_i = [0\ 0\ 1\ 0\ 0\ 0]^{\top}$. In this case the momentum condition (13) imposes

$$\delta I_{xz} = \delta I_{yz} = \delta I_{zz} = \delta h_y = \delta h_x = 0 \tag{15}$$

for the second link. The first three restrictions ($\delta I_{xz} = \delta I_{yz} = \delta I_{zz} = 0$) ensure that the angular momentum about the $\hat{z}_i$ axis will remain unchanged for angular velocities, while the last two $\delta h_y = \delta h_x = 0$ likewise ensure the same for linear velocities. The implication is that, for the second body, I_{xz}, I_{yz}, I_{zz}, h_y, and h_x are identifiable via the joint torque.

Likewise the invariance condition (14) imposes

$$\delta h_y = \delta h_x = \delta I_{xy} = \delta I_{xz} = \delta I_{yz} = \delta I_{xx} - \delta I_{yy} = 0 \tag{16}$$

to ensure that $\delta\mathbf{I}_i$ maps in a fixed way to the parent. Physically, these invariance conditions are satisfied for any mass distribution that is symmetric about the $\hat{z}_i$ axis. Comparing with (15) this implies that I_{xy} and $I_{xx} - I_{yy}$ also affect the dynamics, but via changes in the way these parameters are combined with the parent inertia.

To satisfy both the momentum and invariance considerations, $\delta\mathbf{I}_i$ is left with three degrees of freedom

$$\delta m, \delta h_z, \delta I_{xx} = \delta I_{yy}$$

Notation for this third freedom signifies that changes in I_{xx} must match those to I_{yy}. In this example, the inertia exchange has a physical interpretation. The transfer freedoms represent an exchange of any infinitely thin rod along $\hat{z}_i$.

IV. Two Bodies: Restricted Spatial Motion

Building on the previous section, we explore how spatial motion restrictions affect identifiability. Similar to the previous case, parameters of a body are identified via two mechanisms: (1) directly via how the the parameters are sensed on the preceding joint, or (2) indirectly via variations in how the parameters map to their parent body. However, if the parent has motion restrictions, some of its parameters may not appear in the equations of motion, and thus would be unidentifiable. Thus, for a child parameter to make use of the second identification mechanism, variations in the mapping to the parent must appear on identifiable parameters of the parent. Conversely, an inertial transfer will be unobservable if (1) it cannot be directly sensed on the connecting joint and (2) the transfer maps in a fixed way onto the identifiable parameters of the parent. We develop these conditions mathematically by considering two bodies with motion restrictions and then working through examples.

A. Undetectable Changes in Inertia

In the previous development, body i-1 was considered as experiencing unrestricted movement. This simplified analysis when reducing the conditions for $\delta T = 0$

$$\mathbf{0} \equiv \mathbf{\Phi}_i^{\top}\delta\mathbf{I}_i\mathbf{v}_i \tag{17}$$

$$\mathbf{0} \equiv \mathbf{v}_{i\text{-}1}^{\top}\left[\delta\mathbf{I}_{i\text{-}1} + {}^{i}\mathbf{X}_{i\text{-}1}^{\top}(q_i)\,\delta\mathbf{I}_i\,{}^{i}\mathbf{X}_{i\text{-}1}(q_i)\right]\mathbf{v}_{i\text{-}1} \tag{18}$$

since the body velocities could take any value in $\mathbb{R}^6$. Let us instead consider these conditions in the context where $\mathbf{v}_{i\text{-}1}$ is restricted to some set $\mathcal{V}_{i\text{-}1}^{*}$. The corresponding set of possible velocities for body i is then given by

$$\mathcal{V}_i^{*} = \{{}^{i}\mathbf{X}_{i\text{-}1}(q_i)\,\mathbf{v}_{i\text{-}1} + \mathbf{\Phi}_i\,\dot{q}_i \mid \mathbf{v}_{i\text{-}1} \in \mathcal{V}_i^{*},\ q_i, \dot{q}_i \in \mathbb{R}\} \tag{19}$$

Again, we consider conditions under which the transfer assignment:

$$\delta\mathbf{I}_{i\text{-}1} = -{}^{i}\mathbf{X}_{i\text{-}1}^{\top}(0)\,\delta\mathbf{I}_i\,{}^{i}\mathbf{X}_{i\text{-}1}(0)$$

satisfies the above conditions.

Simplifying the Momentum Condition (17): The condition (17) is impractical to verify as written since it represents an infinite number of constraints. To simplify this condition, consider the following set, which captures the span of the attainable velocities for body i:

$$\mathcal{V}_i = \mathrm{span}\{\mathcal{V}_i^{*}\} \tag{20}$$

This set is a subspace of $\mathbb{R}^6$ and is an alternative characterization of the motion restrictions on body i.

Remark 1. *Note that $\mathcal{V}_i^* \subseteq \mathcal{V}_i$, since not all elements of $\mathcal{V}_i$ need be attainable velocities. Rather, all elements of $\mathcal{V}_i$ can be expressed as the linear combination of some attainable velocities.*

For the time being, let us consider any matrix $\mathbf{V}_i$ such that $\text{Range}(\mathbf{V}_i) = \mathcal{V}_i$. (We will provide methods to compute such a matrix in the following sections.) Using this matrix, (17) is equivalent to $\mathbf{\Phi}_i^\top \delta\mathbf{I}_i \mathbf{V}_i = \mathbf{0}$. Physically, this condition encodes that $\delta\mathbf{I}_i$ must not change the components of body i's momentum associated the joint $\mathbf{\Phi}_i$.

Simplifying Condition (18): Similarly, the conditions (18) are impractical to verify as written due to their dependence on $\mathbf{v}_{i\text{-}1}$ and q_i. While the momentum conditions are related to the direct identifiability of $\delta\mathbf{I}_i$, the ones in (18) are related to the indirect identifiability of $\delta\mathbf{I}_i$ via torques earlier in the mechanism. This indirect nature makes these conditions more challenging to simplify. We proceed to first remove their dependence on q_i before then addressing dependence on $\mathbf{v}_{i\text{-}1}$.

In the spirit of the invariance condition from previously, consider the difference in how the parent views $\delta\mathbf{I}_i$ with changes in configuration:

$$\mathbf{\Delta}_i(q_i) = {}^i\mathbf{X}_{i\text{-}1}^\top(q_i)\, \delta\mathbf{I}_i\, {}^i\mathbf{X}_{i\text{-}1} - {}^i\mathbf{X}_{i\text{-}1}^\top(0)\, \delta\mathbf{I}_i\, {}^i\mathbf{X}_{i\text{-}1}(0) \quad (21)$$

When $\delta\mathbf{I}_i$ satisfies the invariance condition from the previous section, $\mathbf{\Delta}_i(q_i) \equiv \mathbf{0}$, indicating that $\delta\mathbf{I}_i$ maps in a fixed way to the parent. When $\mathbf{\Delta}_i(q_i) \neq \mathbf{0}$, the transfer assignment represents a equal and opposite transfer in the zero configuration, but has some residual as configuration varies. However, as long as this residual maps onto unidentifiable parameters for the parent, we will find that the exchange remains undetectable.

With this definition, (18) is rewritten as

$$0 \equiv \mathbf{v}_{i\text{-}1}^\top\, \mathbf{\Delta}_i(q_i)\, \mathbf{v}_{i\text{-}1} \quad (22)$$

Since the left side of (22) is an analytic function of q_i (i.e., given exactly by its Taylor series), we can enforce that it is zero everywhere by 1) ensuring that it is zero at some point and 2) ensuring that all its derivatives w.r.t. q_i are zero at that point. The condition (22) holds at $q_i = 0$ by virtue of the inertia transfer assignment. Considering the derivatives of (22) requires

$$\frac{\mathrm{d}^{(k)}}{\mathrm{d}q_i^{(k)}} \left[\mathbf{v}_{i\text{-}1}^\top\, {}^i\mathbf{X}_{i\text{-}1}^\top(q_i)\, \delta\mathbf{I}_i\, {}^i\mathbf{X}_{i\text{-}1}(q_i)\, \mathbf{v}_{i\text{-}1}\right]\Bigg|_{q_i=0} = 0,$$

for all positive integers k. We will see that this condition holds when all changes in the way $\delta\mathbf{I}_i$ maps to its parent appear on unidentifiable parameters. Turning this around, $\delta\mathbf{I}_i$ must map in a fixed way onto all identifiable parameters of the parent.

The condition for the k-th derivative is equivalent to:

$$\mathbf{v}_{i\text{-}1}^\top\, {}^i\mathbf{X}_{i\text{-}1}^\top(0)\, \delta\mathbf{I}_i^{(k)}\, {}^i\mathbf{X}_{i\text{-}1}(0)\, \mathbf{v}_{i\text{-}1} = 0 \quad (23)$$

where $\delta\mathbf{I}_i^{(0)} = \delta\mathbf{I}_i$ and

$$\delta\mathbf{I}_i^{(k+1)} = (\mathbf{\Phi}_i\times)^\top\, \delta\mathbf{I}_i^{(k)} + \delta\mathbf{I}_i^{(k)}\, (\mathbf{\Phi}_i\times)$$

The matrix $\delta\mathbf{I}_i^{(k)}$ captures the k-th derivative in how $\delta\mathbf{I}_i$ maps to the parent. The invariance condition is equivalent to the first derivative $\delta\mathbf{I}_i^{(1)}$ satisfying $\delta\mathbf{I}_i^{(1)} = \mathbf{0}$. Each successive derivative is linear in the previous, and thus, for all derivatives after $k = 10$, the condition (23) can be guaranteed to be redundant via the Cayley-Hamilton Theorem [41].

Simplifying the Invariance Condition (23): To further simplify our new invariance condition (23) and make its physical meaning more precise, we will consider the identifiable and unidentifiable parameters of the bodies.

Note that the inertia of body i is linear in parameters $\boldsymbol{\pi}_i$.

$$\boldsymbol{\pi} = [m, h_x, h_y, h_z, I_{xx}, I_{xy}, I_{xz}, I_{yy}, I_{yz}, I_{zz}]^\top$$

To switch between the matrix and parameter vector form of the spatial inertia we employ the notation

I（Pi）是Pi升维成矩阵的形式

$$\mathbf{I}(\boldsymbol{\pi}_i) = [\boldsymbol{\pi}_i]^\wedge \text{ and } \boldsymbol{\pi}_i = [\mathbf{I}(\boldsymbol{\pi}_i)]^\vee \quad (24)$$

where the wedge $\wedge$ promotes a vector to an inertia matrix, while the vee $\vee$ demotes an inertia to a parameter vector.

Using this notation, it follows that there exists a function $\mathbf{k}(\cdot) : \mathbb{R}^6 \to \mathbb{R}^{10}$ such that

$$\frac{1}{2}\mathbf{v}^\top \mathbf{I}_i \mathbf{v} = \frac{1}{2}\mathbf{v}^\top\, [\,\boldsymbol{\pi}_i\,]^\wedge\, \mathbf{v} = \mathbf{k}(\mathbf{v})^\top \boldsymbol{\pi}_i$$

for any $\mathbf{v} \in \mathbb{R}^6$. Intuitively, if $\mathbf{k}(\mathbf{v})^\top \delta\boldsymbol{\pi}_i = 0$ for all $\mathbf{v} \in \mathcal{V}_i^*$, the linear combination of parameters given via $\delta\boldsymbol{\pi}_i$ does not appear in the kinetic energy (i.e., they are unidentifiable).

With this motivation, consider the span of the vectors $\mathbf{k}(\mathbf{v}_i)$ over all attainable velocities for body i:

$$\mathcal{K}_i = \text{span}\{\mathbf{k}(\mathbf{v}_i) \mid \mathbf{v}_i \in \mathcal{V}_i^*\}$$

Analogous to the velocity span $\mathcal{V}_i$, $\mathcal{K}_i$ is a vector subspace of $\mathbb{R}^{10}$ and thus has a finite basis representation. We consider any matrix $\mathbf{K}_i$ with $\text{Range}(\mathbf{K}_i^\top) = \mathcal{K}_i$, with an algorithm to compute $\mathbf{K}_i$ given in the next section. A change $\delta\boldsymbol{\pi}_i$ to body i is unidentifiable if and only if $\mathbf{K}_i\, \delta\boldsymbol{\pi}_i = \mathbf{0}$. Turning this around, it follows that the rows of $\mathbf{K}_i$ form a basis for the inertial parameters of body i that are identifiable themselves or in combination with the parameters of earlier bodies.

Using this matrix, we are finally able to remove the dependence of (23) on $\mathbf{v}_{i\text{-}1}$. We rewrite it as:

$$\mathbf{K}_{i-1} \left[{}^i\mathbf{X}_{i\text{-}1}^\top(0)\, \delta\mathbf{I}_i^{(k)}\, {}^i\mathbf{X}_{i\text{-}1}(0)\right]^\vee = \mathbf{0}, \quad k = 1, \ldots, 10$$

which enforces that $\delta\mathbf{I}_i$ maps in a fixed way onto the identifiable parameters of the parent.

Summary: For systems with motion restrictions, inertia transfers across any joint i are unobservable to the kinetic energy if they satisfy:

$$\mathbf{0} = \mathbf{\Phi}_i \delta\mathbf{I}_i \mathbf{V}_i \quad \text{(Momentum)} \quad (25)$$

$$\mathbf{0} = \mathbf{K}_{i-1} \left[{}^i\mathbf{X}_{i\text{-}1}^\top(0)\, \delta\mathbf{I}_i^{(k)}\, {}^i\mathbf{X}_{i\text{-}1}(0)\right]^\vee \quad \text{(Invariance)} \quad (26)$$

$$\forall k = 1, \ldots, 10$$

B. Example

We work through these conditions within the context of the two 2R manipulators shown in Fig. 3.

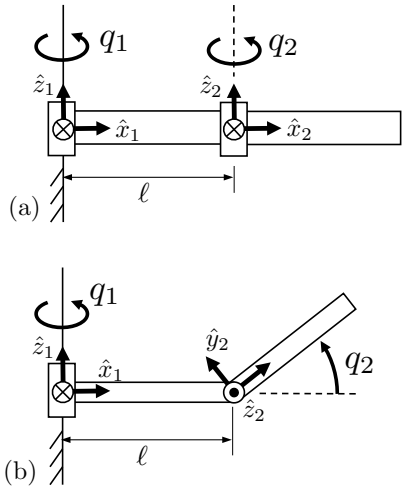

Fig. 3. Two simple RR manipulators.

1) Simple system with parallel joint axes: The system in Figure 3(a) is planar, with the spatial velocities of its bodies and a basis $\mathbf{V}_2$ given by:

$$\mathbf{v}_1 = \begin{bmatrix} 0 \\ 0 \\ \dot{q}_1 \\ 0 \\ 0 \\ 0 \end{bmatrix} \qquad \mathbf{v}_2 = \begin{bmatrix} 0 \\ 0 \\ \dot{q}_1+\dot{q}_2 \\ \ell s_2 \dot{q}_1 \\ \ell c_2 \dot{q}_1 \\ 0 \end{bmatrix} \qquad \mathbf{V}_2 = \begin{bmatrix} 0 & 0 & 0 \\ 0 & 0 & 0 \\ 1 & 0 & 0 \\ 0 & 1 & 0 \\ 0 & 0 & 1 \\ 0 & 0 & 0 \end{bmatrix}$$

where $c_2 = \cos(q_2)$ and $s_2 = \sin(q_2)$. Note that the velocity span for body 2 includes linear velocities in both the x and y directions, since effects from $\dot{q}_1$ will be in the $\hat{x}_2$ or $\hat{y}_2$ direction depending on the value of q_2. The parameter I_{zz_1} is the only inertial parameter for body 1 that affects its kinetic energy and thus:

$$\mathbf{K}_1 = \begin{bmatrix} 0 & 0 & 0 & 0 & 0 & 0 & 0 & 0 & 0 & 1 \end{bmatrix}$$

The momentum condition $\mathbf{0} = \mathbf{\Phi}_2^\top \, \delta \mathbf{I}_2 \, \mathbf{V}_2$ imposes

$$\delta I_{zz_2} = \delta h_{x_2} = \delta h_{y_2} = 0$$

That is, for any velocities in $\mathbf{V}_2$, the change $\delta \mathbf{I}_2$ must not modify the angular momentum of the second body about $\hat{z}_2$. As a result, the three parameters (I_{zz_2}, h_{x_2}, and h_{y_2}) are identifiable via the second joint torque.

The invariance condition (26), written as:

$$0 = \mathbf{K}_1 \, [\, {}^2\mathbf{X}_1^\top(0) \, \delta \mathbf{I}_2^{(k)} \, {}^2\mathbf{X}_1(0) \,]^\vee$$

imposes that the mapping of $\delta \mathbf{I}_2$ onto $I_{zz,1}$ must remain fixed with joint angle. Alternatively, this condition can be written equivalently using (23) as:

$$0 = \mathbf{\Phi}_1^\top, {}^2\mathbf{X}_1^\top(0) \, \delta \mathbf{I}_2^{(k)} \, {}^2\mathbf{X}_1(0) \mathbf{\Phi}_1$$

since $\mathbf{v}_1 = \mathbf{\Phi}_1 \dot{q}_1$. The invariance constraint imposes that $\delta h_{y_2} = 0$ when $k = 1$ and $\delta h_{x_2} = 0$ when $k = 2$. The constraints are redundant for all k higher. Thus h_{y_2} and h_{x_2} are identifiable via variations in how they combine with the identifiable parameter I_{zz_1} of body 1 in the dynamics.

To understand these restrictions physically, note that the inertia $\mathbf{I}_2$ felt about $\hat{z}_1$ is given by:

$$\mathbf{\Phi}_1^\top \, {}^2\mathbf{X}_1^\top \, \mathbf{I}_2 \, {}^2\mathbf{X}_1 \mathbf{\Phi}_1 = I_{zz_2} + m_2 \ell^2 + 2\ell \, h_{x_2} c_2 - 2\ell \, h_{y_2} s_2 \tag{27}$$

The relaxed invariance conditions ensure that variations in how $\delta \mathbf{I}_2$ maps to the identifiable parameter of body 1 (I_{zz_1}) must be zero. More specifically, the condition when $k = 1$ ensures that the first derivative

$$\frac{\mathrm{d}}{\mathrm{d}q_2} \mathbf{\Phi}_1^\top {}^2\mathbf{X}_1^\top \delta \mathbf{I}_2 \, {}^2\mathbf{X}_1 \mathbf{\Phi}_1 = -2\ell \, \delta h_{x_2} s_2 - 2\ell \, \delta h_{y_2} c_2$$

is zero at $q_2 = 0$. Likewise, the condition when $k = 2$ ensures that the second derivative is zero at $q_2 = 0$.

Overall, we see that h_{x_2} and h_{y_2} map in a variable way to the identifiable parameter of body 1, and thus are identifiable indirectly via these changes. Since m_2 and I_{zz_2} map to I_{zz_1} in a fixed way in (27), they not identifiable by themselves, but rather only in combination with I_{zz_1}.

Comparing to the revolute joint momentum and invariance conditions (15) and (16) for the floating-base case, these fixed-base conditions represent a subset. An inertial transfer in the floating-base case has three degrees of freedom, while conditions in this case result in seven transfer degrees of freedom. Overall, the second body has 7 degrees of freedom in its inertia transfer with body 1.

2) Simple system with perpendicular joint axes: For the system in Fig. 3(b), the second body can move out of the $\hat{x}_1 - \hat{y}_1$ plane, resulting in additional motion freedom. A full derivation for this example is in Appendix B, with main results summarized here. The momentum conditions provide:

$$\delta I_{xz_2} = \delta I_{yz_2} = \delta I_{zz_2} = 0 \tag{28}$$

which imply that I_{xz_2}, δI_{yz_2}, and δI_{zz_2} can be identified through the second joint torque. The invariance conditions require:

$$\delta h_{x_2} = \delta h_{y_2} = \delta I_{xx_2} - \delta I_{yy_2} = \delta I_{xy_2} = 0 \tag{29}$$

which imply that h_{x_2}, h_{y_2}, $I_{xx_2} - I_{yy_2}$, and I_{xy_2} can be identified via the first joint torque. Note again, due to motion restrictions, conditions (28) and (29) represent a subset of those in the free-floating case (15) and (16) respectively. However, unlike the previous manipulator with parallel joints, the seven conditions from (28) and (29) are independent. As a result, the unobservable transfers across Joint 2 have three degrees of freedom, which must coincide with those in the free-floating case.

V. Kinematic Chains Of Bodies

This section builds further by using the previous results to characterize identifiability for floating- and fixed-base kinematic chains. We first consider a floating-base serial chain of N bodies connected via single-DoF joints. Extensions to tree-structure systems and multi-DoF joints are discussed in Section VII.

A. Floating-Base Systems

The floating-base case ends up being covered by our the fixed-base theory with multi-DoF joints, so we focus descrip-

tion on intuition here. Parameter changes do not affect the kinetic energy if and only if they do not affect the system mass matrix $\mathbf{H}$. For a floating-base system, consider the liberty of partitioning the generalized velocity as $\dot{\mathbf{q}} = [\mathbf{v}_1^\top \ \dot{\mathbf{q}}_J^\top]^\top$ where $\dot{\mathbf{q}}_J$ gives the vector of joint velocities. The upper triangle of the symmetric mass matrix can then be given by [40]

$$\mathbf{H} = \begin{bmatrix} \mathbf{I}_1^C & {}^2\mathbf{X}_1^\top \mathbf{I}_2^C \boldsymbol{\Phi}_2 & \cdots & {}^N\mathbf{X}_1^\top \mathbf{I}_N^C \boldsymbol{\Phi}_N \\ \cdot & \boldsymbol{\Phi}_2^\top \mathbf{I}_2^C \boldsymbol{\Phi}_2 & \cdots & \boldsymbol{\Phi}_2^\top {}^N\mathbf{X}_2^\top \mathbf{I}_N^C \boldsymbol{\Phi}_N \\ \cdot & \cdot & \ddots & \vdots \\ \cdot & \cdot & \cdot & \boldsymbol{\Phi}_N^\top \mathbf{I}_N^C \boldsymbol{\Phi}_N \end{bmatrix} \tag{30}$$

where $\mathbf{I}_i^C$ is the composite rigid-body inertia [42] of the subchain of bodies rooted at body i. The transfer assignment $\delta\mathbf{I}_{i-1} = -{}^i\mathbf{X}_{i-1}^\top(0)\,\delta\mathbf{I}_i\,{}^i\mathbf{X}_{i-1}(0)$ will leave the composite inertia $\mathbf{I}_{i-1}^C$ unchanged. Since only these composite effects appear within earlier rows of $\mathbf{H}$ in (30), any additional undetectable changes to inertias earlier in the chain $\delta\mathbf{I}_1, \ldots, \delta\mathbf{I}_{i-1}$ can be determined independently. The following theorem states this observation formally.

Theorem 1 (Parameter Nullspace for a Floating-Base System)**.** *Consider a floating-base system and the following inertia transfer subspaces for each joint*

$$\begin{aligned} \mathcal{T}_i = \{\delta\boldsymbol{\pi} \in \mathbb{R}^{10N} \mid \delta\mathbf{I}_{i\text{-}1} &= -{}^i\mathbf{X}_{i\text{-}1}^\top(0)\,\delta\mathbf{I}_i\,{}^i\mathbf{X}_{i\text{-}1}(0), \\ \mathbf{0} &= \boldsymbol{\Phi}_i^\top\,\delta\mathbf{I}_i, \\ \mathbf{0} &= \left[\,(\boldsymbol{\Phi}_i\times)^\top\,\delta\mathbf{I}_i + \delta\mathbf{I}_i\,(\boldsymbol{\Phi}_i\times)\,\right], \\ \mathbf{0} &= \delta\mathbf{I}_j \text{ if } j \notin \{i, i\text{-}1\}\} \end{aligned}$$

for $i = 2, \ldots, N$. The structurally unobservable parameter subspace $\mathcal{N}$ is given by

$$\mathcal{N} = \bigoplus_{i=2}^{N} \mathcal{T}_i$$

where $\bigoplus$ denotes the direct sum of vector subspaces.

Remark 2. *Although gravity has been neglected thus far, its effects provide no additional identifiable parameters in floating-base systems. This result is due to the fact that the floating base can be accelerated opposite gravity to excite the same dynamic effects as does gravity itself.*

Remark 3. *Theorem 1 concerns floating-base systems without motion restrictions. However, for purely floating systems (i.e., those in free flight without any contacts), conservation of linear and angular momentum imposes motion restrictions. In this case, the total mass of the system cannot be identified [6]. Once in contact, however, this unidentifiable parameter combination is no longer present due to the influence of interaction forces on the CoM motion. As a result, systems evolving in and out of contact have parameter identifiability that coincides with the case of unrestricted motion.*

Remark 4. *Note that Ayusawa et al. [6] provide an alternate characterization of identifiability for floating-base system, along with a powerful original result, stated as follows. For a floating-base open-chain system, the inertial parameters that are identifiable through measurement of joint torques and external forces are the same as when joint torques are not available. This result has immediate application to identifying position-controlled robots. As an aside, Appendix D revisits this previous result using the tools considered herein, providing an alternative (and shorter) proof that we hope may help enhance appeal to a broader range of readers.*

B. Fixed-Base Systems

Using the conditions in the previous section, and a companion derivation in Appendix C, we arrive at our main result:

Theorem 2. *(Main Result) Consider a fixed-base system in the absence of gravity, with the following inertia transfer subspaces for each joint ($i \in \{1, \ldots, N\}$):*

$$\begin{aligned} \mathcal{T}_i = \{\delta\boldsymbol{\pi} \in \mathbb{R}^{10N} \mid \delta\boldsymbol{\pi}_0 \in \mathbb{R}^{10}, \\ \delta\mathbf{I}_{i\text{-}1} = -{}^i\mathbf{X}_{i\text{-}1}^\top(0)\,\delta\mathbf{I}_i\,{}^i\mathbf{X}_{i\text{-}1}(0), \\ \mathbf{0} = \mathbf{V}_i^\top\,\delta\mathbf{I}_i\,\boldsymbol{\Phi}_i, \\ \mathbf{0} = \mathbf{K}_{i-1}\left[{}^i\mathbf{X}_{i\text{-}1}^\top(0)\,\delta\mathbf{I}_i^{(k)}\,{}^i\mathbf{X}_{i\text{-}1}(0)\right]^\vee \\ \forall k = 1, \ldots, 10 \\ \mathbf{0} = \delta\mathbf{I}_j \text{ if } j \notin \{i, i\text{-}1\}\ \} \end{aligned}$$

The structurally unobservable parameter subspace $\mathcal{N}$ satisfies

$$\mathcal{N} = \bigoplus_{i=1}^{N} \mathcal{T}_i$$

Proof. The proof follows from induction based on the derivation in Appendix C. □

Remark 5. *The above theorem only applies to the gravity-free case. In fixed-base robots, gravitational forces provide opportunity to identify additional mechanism parameters, decreasing the dimensionality of $\mathcal{N}$. The following section provides a simple method to address these effects within a recursive algorithm.*

VI. Algorithm

This section considers how to compute bases for the the attainable velocity spans $\mathcal{V}_i$, identifiable parameter spans $\mathcal{K}_i$, and transfer subspaces $\mathcal{T}_i$. Recursive application of controllability and observability from linear systems theory plays a key role in computing bases for these sets.

A. Velocity Spans

Bases $\mathbf{V}_i$ for the velocity spans can be computed starting from $\mathbf{V}_0 = \mathbf{0}_{6\times 1}$ and proceeding outward, as in Fig. 4.

Lemma 1. *Suppose a matrix $\mathbf{V}_{i\text{-}1}$ such that $\mathcal{V}_{i\text{-}1} = \mathrm{Range}(\mathbf{V}_{i\text{-}1})$. Let $\mathbf{V}_{i^-} = {}^i\mathbf{X}_{i\text{-}1}(0)\mathbf{V}_{i\text{-}1}$. Then, the matrix*

$$\mathbf{V}_i = [\,\mathrm{Ctrb}(\,(\boldsymbol{\Phi}_i\times), \mathbf{V}_{i^-}\,)\,, \boldsymbol{\Phi}_i\,] \tag{31}$$

satisfies $\mathcal{V}_i = \mathrm{Range}(\mathbf{V}_i)$, where

$$\mathrm{Ctrb}(\,(\boldsymbol{\Phi}_i\times), \mathbf{V}_{i^-}\,) = [\mathbf{V}_{i^-}, (\boldsymbol{\Phi}_i\times)\,\mathbf{V}_{i^-}, \ldots, (\boldsymbol{\Phi}_i\times)^5\,\mathbf{V}_{i^-}]$$

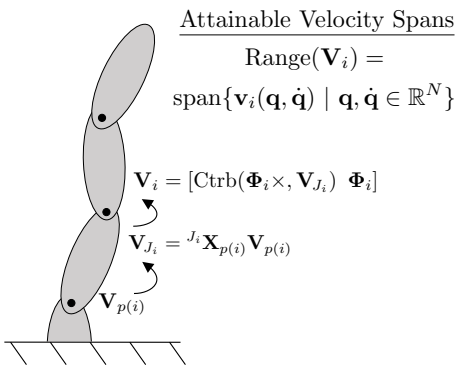

Fig. 4. Controllability analysis is applied recursively to obtain a basis $\mathbf{V}_i$ for the span of the attainable velocities for each body, starting with $\mathbf{V}_0 = \mathbf{0}_{6\times1}$. TODO: Update with new notation

is the controllability matrix [41] associated with the pair $(\,(\mathbf{\Phi}_i\times), \mathbf{V}_{i^-}\,)$.

Proof. See Appendix E. □

To provide intuition into this result, $\mathbf{V}_{i^-}$ first transforms $\mathbf{V}_{i\text{-}1}$ *across the link*. Then $\text{Ctrb}(\,(\mathbf{\Phi}_i\times), \mathbf{V}_{i^-}\,)$ in (31) captures all possible velocity effects from the predecessor following transformation *across the joint*. Then, the second term $\mathbf{\Phi}_i$ adds in effects from the relative velocity of the joint itself.

To express the momentum condition using inertial parameters, we define the matrix:

$$\mathbf{M}(\mathbf{V},\mathbf{\Phi}) = \frac{\partial}{\partial\delta\boldsymbol{\pi}}\mathbf{V}^\top\,[\,\delta\boldsymbol{\pi}\,]^\wedge\,\mathbf{\Phi} \tag{32}$$

Inertia variations $\delta\mathbf{I}_i$ satisfy the momentum condition $\mathbf{V}_i^\top\delta\mathbf{I}_i\mathbf{\Phi}_i = \mathbf{0}$ if and only if the corresponding parameter changes $\delta\boldsymbol{\pi}_i$ satisfy $\mathbf{M}(\mathbf{V}_i,\mathbf{\Phi}_i)\delta\boldsymbol{\pi}_i = \mathbf{0}$.

B. *Identifiable Parameter Spans*

We proceed to simplify the invariance condition (26) for algorithmic implementation. Consider the parameter transformation matrix

$${}^{i\text{-}1}\mathbf{B}_{i^-} = \frac{\partial}{\partial\delta\boldsymbol{\pi}_i}\left[\,{}^i\mathbf{X}_{i\text{-}1}^\top(0)\,[\,\delta\boldsymbol{\pi}_i\,]^\wedge\,{}^i\mathbf{X}_{i\text{-}1}(0)\,\right]^\vee$$

that maps parameters to the predecessor. With this matrix, we can re-express the transfer assignment as:

$$\delta\boldsymbol{\pi}_{i\text{-}1} = -{}^{i\text{-}1}\mathbf{B}_{i^-}\delta\boldsymbol{\pi}_i$$

With this matrix, (26) is equivalent to

$$\mathbf{K}_{i-1}\,{}^{i\text{-}1}\mathbf{B}_{i^-}\left[\delta\mathbf{I}_i^{(k)}\right]^\vee = \mathbf{0} \quad \forall k = 1,\ldots,10 \tag{33}$$

For further simplification, let $\mathbf{K}_{i^-} = \mathbf{K}_{i-1}\,{}^{i\text{-}1}\mathbf{B}_{i^-}$. Also, note that the derivative operation

$$\delta\mathbf{I}_i^{(k+1)} = (\mathbf{\Phi}_i\times)^\top\,\delta\mathbf{I}_i^{(k)} + \delta\mathbf{I}_i^{(k)}(\mathbf{\Phi}_i\times)$$

is linear in $\delta\mathbf{I}_i^{(k)}$. With this observation, we re-express this relationship between $\delta\mathbf{I}_i^{(k+1)}$ and $\delta\mathbf{I}_i^{(k)}$ instead using inertial parameters. Consider the parameter derivative matrix

$$\mathbf{A}(\mathbf{\Phi}_i) = \frac{\partial}{\partial\delta\boldsymbol{\pi}_i}[(\mathbf{\Phi}_i\times)^\top\,[\delta\boldsymbol{\pi}_i]^\wedge + [\delta\boldsymbol{\pi}_i]^\wedge\,(\mathbf{\Phi}_i\times)]^\vee \tag{34}$$

10*10 代码中是怎么设计的？

that provides the rate of change in parameters under joint motions $\mathbf{\Phi}_i$. For example, this matrix satisfies

10*1 6*6 10*3 6*6

$$\mathbf{A}(\mathbf{\Phi}_i)\delta\boldsymbol{\pi}_i = [(\mathbf{\Phi}_i\times)^\top\,\delta\mathbf{I}_i + \delta\mathbf{I}_i\,(\mathbf{\Phi}_i\times)]^\vee$$

It follows that $\left[\delta\mathbf{I}^{(k)}\right]^\vee = \mathbf{A}(\mathbf{\Phi}_i)^k\,\boldsymbol{\pi}_i$. This property enables refactoring of (33) as

$$\mathbf{K}_{i^-}\,\mathbf{A}(\mathbf{\Phi}_i)^k\,\delta\boldsymbol{\pi}_i = \mathbf{0} \quad \forall k = 1,\ldots,10 \tag{35}$$

With these matrices, $\mathbf{K}_i$ can be computed recursively, starting from $\mathbf{K}_0 = \mathbf{0}_{1\times10}$, and propagating outward via the following lemma.

Lemma 2. *Suppose a matrix* $\mathbf{K}_{i-1}$ *such that* $\mathcal{K}_{i-1} = \text{Range}(\mathbf{K}_{i-1}^\top)$. *Then, the matrix*

$$\mathbf{K}_i = \begin{bmatrix}\text{Obs}(\,\mathbf{K}_{i^-},\,\mathbf{A}(\mathbf{\Phi}_i)\,)\\ \mathbf{M}(\mathbf{V}_i,\mathbf{\Phi}_i)\end{bmatrix}$$

satisfies $\mathcal{K}_i = \text{Range}(\mathbf{K}_i^\top)$, *where*

$$\text{Obs}(\mathbf{K}_{i^-},\,\mathbf{A}(\mathbf{\Phi}_i)\,) = \begin{bmatrix}\mathbf{K}_{i^-}\mathbf{A}(\mathbf{\Phi}_i)^0\\ \vdots\\ \mathbf{K}_{i^-}\mathbf{A}(\mathbf{\Phi}_i)^9\end{bmatrix}$$

is the observability matrix associated with the pair $(\mathbf{K}_{i^-},\,\mathbf{A}(\mathbf{\Phi}_i)\,)$.

Proof. See Appendix F. □

Similar to before, $\mathbf{K}_{i^-} = \mathbf{K}_{i\text{-}1}\,{}^{i\text{-}1}\mathbf{B}_{i^-}$ transforms the identifiable parameters of body i-1 *across the link*, while $\text{Obs}(\mathbf{K}_{i^-},\,\mathbf{A}(\mathbf{\Phi}_i)\,)$ then transforms them *across the joint*. Finally, the extra rows $\mathbf{M}(\mathbf{V}_i,\mathbf{\Phi}_i)$ add on additional parameters for body i that can be identified from joint i.

The observability matrix across joint i is denoted as

$$\mathbf{O}_i = \text{Obs}(\,\mathbf{K}_{i^-},\,\mathbf{A}(\mathbf{\Phi}_i)\,)$$

Changes satisfying $\mathbf{O}_i\delta\boldsymbol{\pi}_i = \mathbf{0}$ imply that $\delta\boldsymbol{\pi}_i$ maps onto unidentifiable parameters of the parent for all configurations of the connecting joint. The invariance condition (35) can be written as

$$\mathbf{O}_i\,\mathbf{A}(\mathbf{\Phi}_i)\,\delta\boldsymbol{\pi}_i = \mathbf{0}$$

which enforces that all *changes* in how $\delta\mathbf{I}_i$ is mapped to the parent appear on unobservable parameters of the parent.

C. Summary

An inertia transfer $\delta\boldsymbol{\pi}_{i\text{-}1} = -{}^{i\text{-}1}\mathbf{B}_{i^-}\delta\boldsymbol{\pi}_i$ across joint i is unobservable to the kinetic energy if it satisfies:

$$\boxed{\begin{aligned}\mathbf{M}(\mathbf{V}_i,\mathbf{\Phi}_i)\delta\boldsymbol{\pi}_i &= \mathbf{0} \quad \text{(Momentum)} &(36)\\ \mathbf{O}_i\,\mathbf{A}(\mathbf{\Phi}_i)\,\delta\boldsymbol{\pi}_i &= \mathbf{0} \quad \text{(Invariance)} &(37)\end{aligned}}$$

With these definitions, the transfer subspaces can be written purely using inertial parameters

$$\begin{aligned}\mathcal{T}_i = \{\delta\boldsymbol{\pi} \mid \delta\boldsymbol{\pi}_0 \in \mathbb{R}^{10},\ \delta\boldsymbol{\pi}_{i\text{-}1} = -{}^{i\text{-}1}\mathbf{B}_{i^-}\,\delta\boldsymbol{\pi}_i,\\ \mathbf{0} = \mathbf{N}_i\,\delta\boldsymbol{\pi}_i\\ \mathbf{0} = \delta\boldsymbol{\pi}_j \text{ if } j \notin \{i, i\text{-}1\}\ \}\end{aligned}$$

	Momentum Condition	Invariance Condition
General Form (17),(23)	$\boldsymbol{\Phi}_i^\top \delta\mathbf{I}_i\, \mathbf{v}_i = 0, \;\; \forall \mathbf{v}_i \in \mathcal{V}_i^*$	$\mathbf{v}_{i\text{-}1}^\top \boldsymbol{\Delta}_i(q_i)\mathbf{v}_{i\text{-}1} = 0, \;\; \forall \mathbf{v}_{i\text{-}1} \in \mathcal{V}_{i\text{-}1}^*, q_i \in \mathbb{R}$
Restricted Spatial Motion (25),(26)	$\boldsymbol{\Phi}_i^\top \delta\mathbf{I}_i\, \mathbf{V}_i = \mathbf{0}$	$\mathbf{K}_{i-1}\left[{}^i\mathbf{X}_{i\text{-}1}^\top(0)\,\delta\mathbf{I}_i^{(k)}\,{}^i\mathbf{X}_{i\text{-}1}(0)\right]^\vee = \mathbf{0},\; k = 1, ..., 10$
No Motion Restriction (13), (14)	$\boldsymbol{\Phi}_i^\top \delta\mathbf{I}_i = \mathbf{0}$	$(\boldsymbol{\Phi}_i\times)^\top \delta\mathbf{I}_i + \delta\mathbf{I}_i\,(\boldsymbol{\Phi}_i\times) = \mathbf{0}$
Description w/Parameters (36), (37)	$\mathbf{M}(\mathbf{V}_i, \boldsymbol{\Phi}_i)\delta\boldsymbol{\pi}_i = \mathbf{0}$	$\mathbf{O}_i\,\mathbf{A}(\boldsymbol{\Phi}_i)\delta\boldsymbol{\pi}_i = \mathbf{0}$

TABLE II
SUMMARY OF OF CONDITIONS FOR A PARAMETERS TRANSFER AT JOINT i TO BE UNOBSERVABLE TO THE KINETIC ENERGY.

where the transfer nullspace descriptor $\mathbf{N}_i$ is given by

$$\mathbf{N}_i = \begin{bmatrix} \mathbf{M}(\mathbf{V}_i, \boldsymbol{\Phi}_i) \\ \mathbf{O}_i\,\mathbf{A}(\boldsymbol{\Phi}_i) \end{bmatrix}$$

Recall that the rows of $\mathbf{K}_i$ characterize the parameters of body i that are identifiable in combination with the parameters of body i and previous bodies. By comparison, the rows of $\mathbf{N}_i$ characterize the parameters of body i that are identifiable in combination with others of body i alone. In summary, Lemmas 1 and 2 provide the main recursive steps for computing the transfer subspaces across each joint, with the transfer nullspace descriptors $\mathbf{N}_i$ then characterizing each set of undetectable transfers $\mathcal{T}_i$.

D. Addressing Gravity

Within rigid-body dynamics algorithms, effects of gravity are often addressed by fictitiously accelerating the base opposite gravity. This trick is applied in the Recursive Newton-Euler algorithm [43] for inverse dynamics and the articulated-body algorithm for forward dynamics [40]. The same approach also works to address gravitational effects for identifiability. By seeding $\mathbf{V}_0 = {}^0\mathbf{a}_g$, with ${}^0\mathbf{a}_g$ the gravity acceleration in the world coordinate, the recursive computations of this section result in modified transfer subspaces $\mathcal{T}_i$ that include gravitational considerations. Intuitively, this modification corresponds to adding a fictitious prismatic joint aligned with gravity at the base whose force is not measured. Appendix G rigorously analyzes the role of gravity on identifiability and further justifies this simple modification.

E. Algorithm Summary

Algorithm 1 provides a compact method to recursively compute the parameter nullspace descriptors $\mathbf{N}_i$. We name this method the Recursive Parameter Nullspace Algorithm (RPNA). As a practical matter, linearly dependent columns of $\mathbf{V}_i$ or linearly dependent rows of $\mathbf{K}_i$ can be removed at any step in the algorithm. A MATLAB implementation of the RPNA is provided open source at the following link: https://github.com/pwensing/RPNA.

Remark 6. *One might be interested in considering the nullspace under static experiments. An algorithm for the nullspace in this case could be obtained by modifying line 3 of the RPNA to* $\mathbf{V}_i = \left[\mathrm{Ctrb}((\boldsymbol{\Phi}_i\times), {}^i\mathbf{X}_{i\text{-}1}(0)\,\mathbf{V}_{i\text{-}1})\right]$ *which intuitively removes local joint velocities from consideration. See Appendix G for justification.*

Algorithm 1: Recursive Parameter Nullspace Algorithm

1 $\mathbf{V}_0 = {}^0\mathbf{a}_g, \;\; \mathbf{K}_0 = \mathbf{0}_{1\times 10}$
2 **for** $i = 1, \ldots, N$ **do**
3 $\quad \mathbf{V}_{i^-} = {}^i\mathbf{X}_{i\text{-}1}(0)\,\mathbf{V}_{i\text{-}1}$
4 $\quad \mathbf{V}_i = [\mathrm{Ctrb}((\boldsymbol{\Phi}_i\times), \mathbf{V}_{i^-})\;\; \boldsymbol{\Phi}_i]$
5 $\quad \mathbf{K}_{i^-} = \mathbf{K}_{i-1}\,{}^{i\text{-}1}\mathbf{B}_{i^-}$
6 $\quad \mathbf{O}_i = \mathrm{Obs}(\mathbf{K}_{i^-}, \mathbf{A}(\boldsymbol{\Phi}_i))$
7 $\quad \mathbf{K}_i = \begin{bmatrix} \mathbf{M}(\mathbf{V}_i, \boldsymbol{\Phi}_i) \\ \mathbf{O}_i \end{bmatrix}$
8 $\quad \mathbf{N}_i = \begin{bmatrix} \mathbf{M}(\mathbf{V}_i, \boldsymbol{\Phi}_i) \\ \mathbf{O}_i\,\mathbf{A}(\boldsymbol{\Phi}_i) \end{bmatrix}$
9 **end**
10 **return** $\mathbf{N}_i, \quad i = 1, \ldots, N$

Remark 7. *The RPNA has expressed the unobservable parameters through a direct sum of local transfers. The nullspace descriptors* $\mathbf{N}_i$ *can also be used to compute bases for the system-wide parameter nullspace* $\mathcal{N}$ *and its orthogonal complement* $\mathcal{N}^\perp$*. Details are provided in Appendix H. Any basis for* $\mathcal{N}$ *gives the unidentifiable parameter combinations for the mechanism, while any basis for* $\mathcal{N}^\perp$ *gives identifiable parameter combinations.*

VII. EXTENSIONS

A. Tree-Structure Systems

The inertia transfer concept readily generalizes to branched open-chain rigid-body systems. In branched systems, each body has a predecessor, denoted $p(i)$, toward the base. The transfer condition is re-written as

$$\delta\mathbf{I}_{p(i)} = -{}^i\mathbf{X}_{p(i)}^\top(0)\,\delta\mathbf{I}_i\,{}^i\mathbf{X}_{p(i)}(0)$$

All recursive steps of the RPNA generalize to branched systems by likewise replacing $i-1$ with $p(i)$.

B. Multi-DoF Joints

Suppose each joint i has n_{d_i} DoFs with free modes:

$$\mathbf{\Phi}_i = \begin{bmatrix} \boldsymbol{\phi}_{i,1} & \cdots & \boldsymbol{\phi}_{i,n_{d_i}} \end{bmatrix}$$

where each $\boldsymbol{\phi}_{i,j} \in \mathbb{R}^6$ is fixed. For a floating-base system, invariance is generalized for all joint rates by enforcing

$$\mathbf{0} = (\boldsymbol{\phi}_{i,j}\times)^\top \delta\mathbf{I}_i + \delta\mathbf{I}_i\,(\boldsymbol{\phi}_{i,j}\times) \quad \forall j \in \{1,\ldots,n_{d_i}\}$$

The momentum and transfer conditions generalize directly.

For a fixed-base system, additional modifications are required to accommodate multi-DoF joints. First, the propagation of the attainable velocity spans must be generalized. For a single-DoF joint, joint kinematics follow a linear system (**??**). In contrast, for a multi-DoF joint:

$$\frac{\mathrm{d}}{\mathrm{d}t}{}^i\mathbf{X}_{p(i)}(\mathbf{q}_i) \in \operatorname{span}\left((\boldsymbol{\phi}_{i,1}\times){}^i\mathbf{X}_{p(i)}, \ldots, (\boldsymbol{\phi}_{i,n_{d_i}}\times){}^i\mathbf{X}_{p(i)}\right)$$

As a result, the span

$$\operatorname{span}\{\mathbf{v} \mid \exists \mathbf{q}_i, \mathbf{v} \in \operatorname{Range}({}^i\mathbf{X}_{p(i)}(\mathbf{q}_i)\,\mathbf{V})\}$$

can be seen as the smallest set containing $\operatorname{Range}(\mathbf{V})$ that is invariant under each $(\boldsymbol{\phi}_{i,k}\times)$. This set is equivalent to the controllable subspace of a switched linear system [44] with pairs $\{\,(\,(\boldsymbol{\phi}_{i,k}\times), \mathbf{V}\,)\,\}_{k=1}^{n_{d_i}}$. If the controllability matrix in Lemma 1 is replaced by a matrix whose range equals the switched controllable subspace of these pairs, then Lemma 1 holds more generally. Likewise, observability conditions in Lemma 2 generalize to multi-DoF joints using observability for switched linear systems.

C. Closed Kinematic Loops: Joint Motors

Motor rotors present a simple and common closed kinematic loop, as any motor at joint i is attached both to body $i-1$ and body i. Toward understanding this case, we consider a three-body system with a floating base (body 1), a motor (Body m), and an additional body (body 2).

The mass matrix for this system is given by

$$\mathbf{H} = \begin{bmatrix} \mathbf{I}_1^C & {}^m\mathbf{X}_1^\top\,\mathbf{I}_m\,\mathbf{\Phi}_m\,n_R + {}^2\mathbf{X}_1^\top\,\mathbf{I}_2\,\mathbf{\Phi}_2 \\ \cdot & \mathbf{\Phi}_m^\top\mathbf{I}_m\,\mathbf{\Phi}_m\,n_R^2 + \mathbf{\Phi}_2^\top\,\mathbf{I}_2\,\mathbf{\Phi}_2 \end{bmatrix}$$

where n_R the gear ratio and the composite inertia

$$\mathbf{I}_1^C = \mathbf{I}_1 + {}^m\mathbf{X}_1^\top\,\mathbf{I}_m\,{}^m\mathbf{X}_1 + {}^2\mathbf{X}_1^\top\mathbf{I}_2\,{}^2\mathbf{X}_1$$

Inertia transfer, momentum, and invariance conditions are generalized respectively as

$$\begin{aligned} \delta\mathbf{I}_1 &= -{}^{J_m}\mathbf{X}_1^\top\,\delta\mathbf{I}_m\,{}^{J_m}\mathbf{X}_1 - {}^{J_2}\mathbf{X}_1^\top\delta\mathbf{I}_2\,{}^{J_2}\mathbf{X}_1 \\ \mathbf{0} &= {}^{J_m}\mathbf{X}_1^\top\,\delta\mathbf{I}_m\,\mathbf{\Phi}_m\,n_R + {}^{J_2}\mathbf{X}_1^\top\,\delta\mathbf{I}_2\,\mathbf{\Phi}_2 \end{aligned} \tag{38}$$

$$\begin{aligned} \mathbf{0} = {}&{}^{J_m}\mathbf{X}_1^\top\left[(\mathbf{\Phi}_m\times)^\top\delta\mathbf{I}_m + \delta\mathbf{I}_m(\mathbf{\Phi}_m\times)\right]{}^{J_m}\mathbf{X}_1 n_R \\ &+ {}^{J_2}\mathbf{X}_2^\top\left[(\mathbf{\Phi}_2\times)^\top\delta\mathbf{I}_2 + \delta\mathbf{I}_2(\mathbf{\Phi}_2\times)\right]{}^{J_2}\mathbf{X}_1 \end{aligned} \tag{39}$$

These conditions guarantee that the variation to the first block row of $\mathbf{H}$ is zero. However, unlike the open-chain floating-base case, a zero variation to the first block row does not imply a zero variation to $\mathbf{H}$ overall.[2] Ensuring $\delta\mathbf{H}_{22} = 0$ requires

$$0 = \mathbf{\Phi}_m^\top\,\delta\mathbf{I}_m\,\mathbf{\Phi}_m\,n_R^2 + \mathbf{\Phi}_2^\top\,\delta\mathbf{I}_2\,\mathbf{\Phi}_2 \tag{40}$$

which we refer to as the torque condition.

In the common case that motor rotors are rotationally symmetric, these conditions simplify a great deal. Consider a motor rotating about its z axis such that $\mathbf{\Phi}_m = [0,0,1,0,0,0]^\top$. Rotational symmetry of the rotor implies $I_{xz} = I_{yz} = h_x = h_y = 0$ and $I_{xx} = I_{yy}$. Intuitively, variations respecting this symmetry satisfy

$$\mathbf{0} = (\mathbf{\Phi}_m\times)^\top\delta\mathbf{I}_m + \delta\mathbf{I}_m(\mathbf{\Phi}_m\times)$$

Thus, the momentum (38), transfer invariance (39), and torque (40) conditions simplify to

$$\mathbf{0} = {}^{J_m}\mathbf{X}_1^\top\mathbf{\Phi}_m\,\delta I_{zz_m}\,n_R + {}^{J_2}\mathbf{X}_1^\top\,\delta\mathbf{I}_2\,\mathbf{\Phi}_2 \tag{41}$$

$$\mathbf{0} = (\mathbf{\Phi}_2\times)^\top\delta\mathbf{I}_2 + \delta\mathbf{I}_2(\mathbf{\Phi}_2\times)$$

$$0 = \delta I_{zz_m}\,n_R^2 + \mathbf{\Phi}_2^\top\,\delta\mathbf{I}_2\,\mathbf{\Phi}_2 \tag{42}$$

Since δI_{zz_m} is the only parameter appearing for the motor, it can add one additional identifiable parameter at most. However, there are conditions when the rotor inertia cannot be identified. The only way (41) and (42) can be satisfied simultaneously is if

$$\begin{aligned} \mathbf{\Phi}_2^\top{}^{J_m}\mathbf{X}_{J_2}^\top\mathbf{\Phi}_m\,\delta I_{zz_m}\,n_R + \mathbf{\Phi}_2^\top\delta\mathbf{I}_2\,\mathbf{\Phi}_2 &= \mathbf{0} \\ \delta I_{zz_m}\,n_R^2 + \mathbf{\Phi}_2^\top\,\delta\mathbf{I}_2\,\mathbf{\Phi}_2 &= \mathbf{0} \end{aligned}$$

These equations can be satisfied (and I_{zz_m} is not identifiable) when the gear ratio is unity, Joint 2 is rotational, and its axis is parallel to the motor axis. Note that this condition allows the motor to be offset from the joint. In all other cases, the rotor adds one identifiable parameter I_{zz_m}.

More generally, the fixed-base case requires considerations of motion restrictions to determine whether a single additional motor parameter is identifiable at each joint. The mathematics of these generalizations are omitted here, but are implemented in the attached code.

The main conceptual difference in the fixed-base case is that the motor inertia is only identifiable if it can be felt earlier in the chain. For instance, consider the simple manipulators in Fig. 3 and suppose each motor rotates along the local $\hat{z}_i$ axis. The inertia of the first motor is not felt earlier in the chain for either mechanism (since there are no previous joints), and thus it does not add an identifiable parameter. For the system with parallel joints in Fig. 3(a), the rotational inertia of second motor about its axis does contribute rotational inertia about the first joint axis, and so it adds an identifiable parameter. For the system with perpendicular joint axes, the rotational inertia of the second motor rotor does not lead to any rotational inertia about the first joint axis. Thus neither motor inertia contributes an identifiable parameter in this case.

[2]Relating back to Sec. D, an implication here is that motor rotors are generally not identifiable from ground forces alone.

VIII. Verification and System-Level Examples

This section provides verification of the Recursive Parameter Nullspace (RPNA) for fixed- and floating-base systems. The RPNA is unique in that it requires only the structural parameters of the mechanism as its input, is provably correct, and does not rely on any symbolic manipulations or assumed exciting input data. We use numerical approaches such as SVD [1] to empirically verify the RPNA output.

A. PUMA 560

We first consider the classical industrial manipulator PUMA 560 shown in Figure 5. Coordinate systems follow the Denavit-Hartenberg convention as in [45]. The mechanism has three joints to position the wrist, followed by three wrist joints with intersecting orthogonal axes.

Table III details the parameter identifiability for this mechanism. There are three possibilities for each parameter: identifiable, unidentifiable, and identifiable in linear combinations only [1]. Unidentifiable parameters do not affect the measurements at all. For body i parameter k, this means its corresponding unit vector $\mathbf{e}_{ik} \in \mathbb{R}^{10N}$ satisfies $\mathbf{e}_{ik} \in \mathcal{N}$. Likewise, an identifiable parameter is one that is uniquely determined from maximally exciting data, and is characterized mathematically by $\mathbf{e}_{ik} \in \mathcal{N}^{\perp}$. Remaining parameters (i.e., those that are not individually identifiable or unidentifiable) are identifiable in linear combinations with other parameters only. For instance, while I_{xx_6} and I_{yy_6} cannot be identified alone, $I_{xx_6} - I_{yy_6}$ can be.

A minimal set of parameters representing identifiable combinations is indicated with symbols (☆) in the table. With this designation, the total number of stars in any given column represents the number of identifiable parameter combinations contributed by that body. The number of entries without stars for each body indicates the number of degrees of freedom in the inertia transfer with its parent. Using the RPNA, the PUMA is found to have 36 identifiable parameter combinations for its bodies. This is confirmed by previous symbolic approaches [10], [11]. Additional details on the identifiable linear combinations can be obtained from the supplementary MATLAB code.

Motion restrictions play an important role on the structure of the identifiable parameters for the first two bodies of the PUMA. The true attainable velocity spans have sub-maximal dimensions 1 and 3, and have dimensions 2 and 5 within the algorithm when considering gravity as a fictitious prismatic joint at the base. All remaining bodies have full dimension for $\mathcal{V}_i$ and $\mathcal{K}_i$. Despite the motion restrictions on body 2, its undetectable transfers coincide with that of an unconstrained body. The mass m_2 is unidentifiable since it is not sensed by joint 2, and it is mapped onto the parent parameter m_1, which is itself unidentifiable. Likewise, mc_{z_2} is not sensed by torques on joint 2 and maps to parent parameters mc_{x_1} and mc_{y_1} depending on the value of q_2. Both of these parameters of the parent are unidentifiable, and thus so is mc_{z_2}. With respect to the motor inertias, the first two joints of the PUMA are perpendicular and thus its first two motor inertias are not identifiable as in the simple system from Section IV-B2.

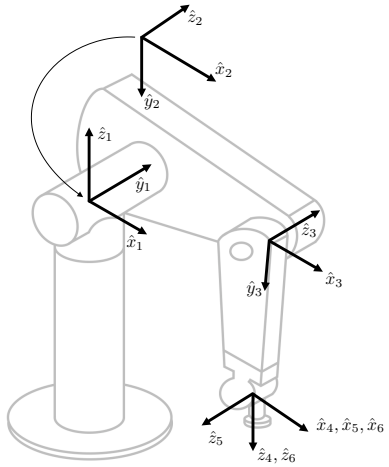

Fig. 5. PUMA 560 robot and coordinate assignment.

	1	2	3	4	5	6
m	×	×				
mc_x	×	☆	☆	★	★	★
mc_y	×	★	☆	☆	☆	★
mc_z	×	×				
I_{xx}	×	☆	☆	☆	☆	☆
I_{yy}	×					
I_{zz}	☆	☆	☆	☆	☆	★
I_{yz}	×	★	★	★	★	★
I_{xz}	×	☆	★	★	★	★
I_{xy}	×	★	☆	★	★	★
I_m			★	★	★	★
$\dim(\mathcal{V}_i)$	1 (2)	3 (5)	6	6	6	6
$\dim(\mathcal{K}_i)$	1 (1)	6 (8)	10	10	10	10
$\dim(\mathcal{T}_i)$	9	3	3	3	3	3

TABLE III
PUMA 560 IDENTIFIABLE (★) AND UNIDENTIFIABLE (×) PARAMETERS. A MINIMAL PARAMETER SET IS INDICATED (☆). UNMARKED ENTRIES ARE ONLY IDENTIFIABLE IN LINEAR COMBINATIONS WITH ☆-TYPE PARAMETERS. NUMBERS IN PARENTHESES INDICATE THE DIMENSION OF THE SET WITHIN THE ALGORITHM WHEN CONSIDERING GRAVITATIONAL EFFECTS.

B. SCARA

The second example considered is a SCARA robot depicted in Fig. 6. The SCARA is a 4-DoF RRPR manipulator traditionally used in pick and place operations. All rotations and translations take place about the local $\hat{z}_i$ axes. Motion restrictions play a key role in parameter observability for this robot as described in Table IV.

Each of the joints in the SCARA admits more transfer freedoms than in the floating case. The first two links of the SCARA resemble the parallel joint example from Section IV-B1. As a result, the second revolute joint admits 7 transfer degrees of freedom and contributes 3 identifiable parameter combinations. Motion restrictions likewise enlarge the undetectable transfers across the prismatic joint. While a free-floating prismatic joint admits 6 transfer degrees of freedom, the SCARA prismatic joint admits 9 transfer degrees of freedom.

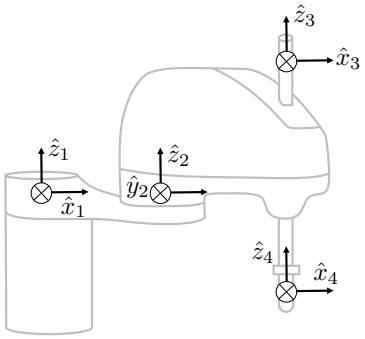

Fig. 6. SCARA robot and coordinate assignment.

	1(R)	2(R)	3(P)	4(R)
m	×		☆	
mc_x	×	☆		★
mc_y	×	☆		★
mc_z	×	×	×	×
I_{xx}	×	×	×	×
I_{yy}	×	×	×	×
I_{zz}	☆	☆		★
I_{yz}	×	×	×	×
I_{xz}	×	×	×	×
I_{xy}	×	×	×	×
I_m		★	★	★
$\dim(\mathcal{V}_i)$	1 (2)	3 (4)	4 (4)	4 (4)
$\dim(\mathcal{K}_i)$	1 (1)	4 (4)	4 (4)	4 (4)
$\dim(\mathcal{T}_i)$	9	7	9	7

TABLE IV
SCARA IDENTIFIABLE (★) AND UNIDENTIFIABLE (×) PARAMETERS. A MINIMAL PARAMETER SET IS INDICATED (☆). UNMARKED ENTRIES ARE ONLY IDENTIFIABLE IN LINEAR COMBINATIONS WITH ☆-TYPE PARAMETERS. NUMBERS IN PARENTHESES INDICATE THE DIMENSION OF THE SET WITHIN THE ALGORITHM WHEN CONSIDERING GRAVITATIONAL EFFECTS.

These extra transfer freedoms for the SCARA prismatic joint can be understood physically from the momentum and invariance conditions. The momentum condition $\mathbf{V}_3^T \delta\mathbf{I}_3 \mathbf{\Phi}_3 = \mathbf{0}$ requires that $\delta\mathbf{I}_3$ must not modify the linear momentum of body 3 along $\hat{z}_3$. Motions of joint 3 will create pure linear momentum along $\hat{z}_3$ with magnitude $m_3\dot{q}_3$, while motions of joints 1 and 2 do not create any linear momentum in this direction. Thus, the momentum condition requires $\delta m_3 = 0$.

It turns out that the invariance condition (**??**) for joint 3 holds without restriction on $\delta\mathbf{I}_3$. Recall that the invariance condition considers changes in the way $\delta\mathbf{I}_3$ maps to parameters of its parent. It holds when any changes in this mapping with q_3 appear only on the unidentifiable parameters for the parent. Changes in q_3 affect the vertical distribution of mass for body 3 relative to its parent. Yet, any of the parameters affected by the vertical distribution of mass (i.e., mc_z, I_{xx}, I_{yy}, I_{xz}, I_{yz}) are unobservable for body 2. Thus, the invariance condition holds without any restriction on $\delta\mathbf{I}_3$. As a result, transfers between body 2 and body 3 need only satisfy the momentum condition $\delta m_3 = 0$, providing 9 transfer freedoms across this joint. Discounting motors, the mechanism has 32 unobservable parameter combinations and therefore only 8 identifiable parameter combinations. This was confirmed empirically through an SVD applied to random samples of the regressor $\mathbf{Y}$.

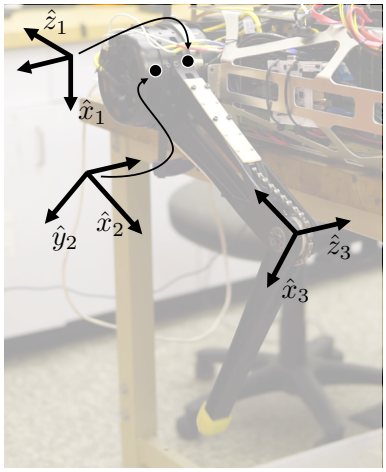

Fig. 7. Cheetah 3 Leg Coordinates. Table-top experiments like the one shown are often used to identify leg parameters.

C. Cheetah 3 Leg

The last example considered is a leg for the MIT Cheetah 3 robot as shown in Figure 7. The full system consists of four legs and a body with 12 DoFs driven by proprioceptive actuators [46]. A common approach is to identify the legs in a procedure separate from the body [25], [33], with the legs identified using fixed-base leg swing experiments as depicted in the figure. We explore whether this common setup is an appropriate method to fully identify the leg, finding that in fact, the motion restrictions in the fixed experiments do not excite all the parameters affecting the dynamics in the floating-base case.

Table V compares the parameter identifiability with the fixed- vs. floating-base case. Similar to the PUMA and SCARA examples, the Cheetah 3 leg model possesses unidentifiable parameters in the fixed-base case. The first two joints of the Cheetah are orthogonal, similar to the PUMA. However, unlike the PUMA, the first joint axis is not aligned with gravity in the test configuration. This provides additional identifiable parameters for the first link in comparison to the PUMA. Again, via arguments similar to the PUMA, the rotational inertia of the rotors on the first two joints are only identifiable in combination with the rotational inertia of their associated successor link. Via comparison, in the floating-base case, the addition of coupling moments onto the body allows a disambiguation between theses two effects, as reflected inertia scales with a factor n_R^2 of the gear ratio n_R on the joint, whereas the associated coupling moments on the body only scale as n_R.

To analyze the effects of motion restrictions in a concrete situation, we consider the case of Cheetah 3 executing a transverse gallop. Ground-truth data is collected in simulation, shown in Figure 8, and includes the configuration

	Fixed			Free		
	1	2	3	1	2	3
m	×					
mc_x	★	☆	★	★	☆	★
mc_y	☆	★	★	☆	★	★
mc_z	×					
I_{xx}	×	☆	☆	☆	☆	☆
I_{yy}	×					
I_{zz}	☆	☆	★	☆	☆	★
I_{yz}	×	★	★	★	★	★
I_{xz}	×	☆	★	★	★	★
I_{xy}	×	★	★	★	★	★
I_m			★	★	★	★
$\dim(\mathcal{V}_i)$	1 (3)	3 (6)	6	6	6	6
$\dim(\mathcal{K}_i)$	1 (3)	6 (9)	10	10	10	10
$\dim(\mathcal{T}_i)$	7	3	3	3	3	3

TABLE V

CHEETAH 3 IDENTIFIABLE (★) AND UNIDENTIFIABLE (×) PARAMETERS. A MINIMAL PARAMETER SET IS INDICATED (☆). UNMARKED ENTRIES ARE ONLY IDENTIFIABLE IN LINEAR COMBINATIONS WITH ☆-TYPE PARAMETERS. NUMBERS IN PARENTHESES INDICATE THE DIMENSION OF THE SET WITHIN THE ALGORITHM WHEN CONSIDERING GRAVITATIONAL EFFECTS.

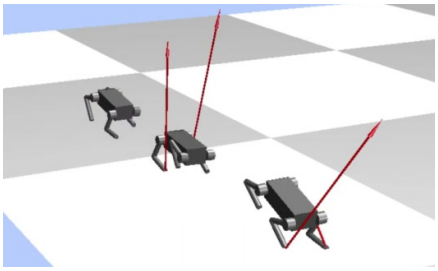

Fig. 8. Full dynamic simulation of galloping was used to obtain the identification dataset for the MIT Cheetah 3 model.

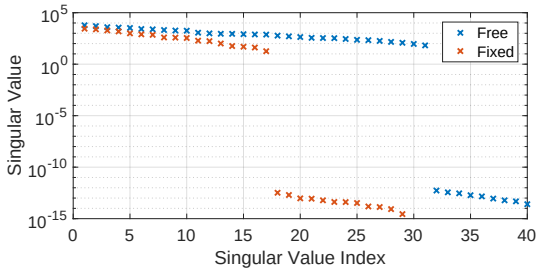

Fig. 9. Singular values for identifying leg and body parameters. A fixed-base experiment enables identification of 17 combinations of parameters for the leg, while the free case enables identification of 31 parameter combinations for the leg and body, 21 of which are for the leg only.

$\mathbf{q}$, generalized velocity $\dot{\mathbf{q}} \in \mathbb{R}^{18}$, generalized acceleration $\ddot{\mathbf{q}} \in \mathbb{R}^{18}$, and generalized force $\boldsymbol{\tau} \in \mathbb{R}^{18}$ during this galloping motion. The generalized force includes effects from both active joint torques as well as effects from ground reaction forces. Collecting this rich dataset would generally be impractical, as it would require precisely calibrated force plates in strategic locations during galloping. However, measurement of all contact forces is necessary to fully identify its dynamics.

We consider two variations of the system identification setup. In a first variation, all the measured data is used to determine an estimate $\hat{\boldsymbol{\pi}} \in \mathbb{R}^{250}$ of the inertial parameters (13 bodies and 12 rotors, each with 10 parameters). Motor-rotors are modeled as rigid-bodies themselves connected to the preceeding link via a revolute joint. The parameters of the system are then found via solving a least-squares problem:

$$\min_{\hat{\boldsymbol{\pi}}} \sum_{j=1}^{N_s} \left\| \begin{bmatrix} \mathbf{0} \\ \boldsymbol{\tau}_J^{[j]} \end{bmatrix} + \mathbf{J}\left(\mathbf{q}^{[j]}\right)^\top \mathbf{f}^{[j]} - \mathbf{Y}\left(\mathbf{q}^{[j]}, \dot{\mathbf{q}}^{[j]}, \ddot{\mathbf{q}}^{[j]}\right) \hat{\boldsymbol{\pi}} \right\|^2 \tag{43}$$

where N_s is the number of samples used, and the superscript $(\cdot)^{[j]}$ indicates the j-th sample of the quantity. Note that this experiment captures both torques for the legs at the joints, as well as associated dynamic coupling forces on the body.

In a second variation, a fixed-base situation is considered mimicking the table-top setup in Figure 7. For simplicity, only the front-left (FL) leg is considered. To provide a fair comparison with the floating-base gallop data set, the same swing-leg trajectories are employed. Samples of the front-left leg configuration $\mathbf{q}_{FL} \in \mathbb{R}^3$, velocity $\boldsymbol{\nu}_{FL} = \dot{\mathbf{q}}_{FL}$, and acceleration $\dot{\boldsymbol{\nu}}_{FL} = \ddot{\mathbf{q}}_{FL}$ are used with ground-truth simulation inertial parameters to generate required joint torques $\boldsymbol{\tau}_{FL} \in \mathbb{R}^3$. It is emphasized that this data is synthetic (i.e., not from physical experiments) in order to provide a fair comparison between mock table-top and floating-base identification experiments.

This synthetic table-top data is used to solve for leg inertial parameters $\hat{\boldsymbol{\pi}}_{FL} \in \mathbb{R}^{60}$ of the front-left leg (3 bodies and 3 rotors) via a similar least-squares problem.

$$\min_{\hat{\boldsymbol{\pi}}_{FL}} \sum_{j=1}^{N_s} \left\| \boldsymbol{\tau}_{FL}^{[j]} - \mathbf{Y}_{FL}\left(\mathbf{q}_{FL}^{[j]}, \boldsymbol{\nu}_{FL}^{[j]}, \dot{\boldsymbol{\nu}}_{FL}^{[j]}\right) \hat{\boldsymbol{\pi}}_{FL} \right\|^2 \tag{44}$$

Due to parameter observability considerations, both (43) and (44) are degenerate least-squares problems with multiple solutions. In practice, regularization strategies are often used with a prior estimate (often from CAD) (e.g., [9]).

To remove any bias from the accuracy of such prior knowledge, unique solutions $\hat{\boldsymbol{\pi}}$ and $\hat{\boldsymbol{\pi}}_{FL}$ were obtained with a pseudo-inverse. Figure 9 shows the singular values for the portion of the regressor that includes the front left leg and body parameters in both the fixed and free cases. The fixed base includes 17 identifiable combinations, while the free case includes 31 identifiable combinations, 21 of which are for the leg only, and 10 of which include the floating-base parameters. The provably-correct output of the RPNA, summarized in Table V, thus certifies that these datasets are maximally exciting for both the fixed- and floating-base cases. Details on the identifiable combinations for both cases are available by running the supplementary MATLAB code.

Table VI shows the validation error in various cases following identification with these two setups. For identification with the full floating-base model, validation errors are zero in both the floating-base and fixed-base validation cases. This is intuitively as expected, since the floating-base dynamics capture a fixed-base constraint as a special setting. In contrast,

	Fixed-Base Validation	**Floating-Base Validation**		
	Leg Torques	Leg Torques	Body Torques	Body Forces
Floating-Base ID	$[0, 0, 0]$ Nm	$[0, 0, 0]$ Nm	$[0, 0, 0]$ Nm	$[0, 0, 0]$ N
Fixed-Base ID	$[0, 0, 0]$ Nm	$[1.36, 2.28, 0.00]$ Nm	$[6.64, 20.23, 4.25]$ Nm	$[15.65, 11.00, 59.63]$ N

TABLE VI

RMS VALIDATION ERRORS ON THE GALLOPING DATASET USING FIXED-BASE VS. FLOATING-BASE IDENTIFICATION. LEG TORQUE VECTOR REPORT AB/AD, HIP, AND KNEE RESIDUALS. FORCE AND TORQUE RESIDUALS ARE REPORTED IN BODY COORDINATES WITH $+x$ FORWARD, $+y$ LEFT, AND $+z$ UP.

the fixed-base identification only displays favorable generalization when applied to another fixed-base data set. When the identified leg model is used within a full floating-base model, validation errors appear on both the leg torques and on the coupling forces/torques.

The parameter observability analysis in Table V explains the leg torque errors in the floating-base validation. These validation errors occur when motions of the body excite new dynamic effects for the leg that were not captured in the mock table-top experiments. It is observed that these motion restrictions are only on the first two links (ab/ad and hip), while the shank (body 3) experiences unrestricted motion as signified by $\dim(\mathcal{V}_3) = 6$ and $\dim(\mathcal{K}_3) = 10$. As a result of this full excitation of the shank parameters in the fixed-base case, the knee joint experiences zero validation errors when generalizing to the free-base case.

Validation errors for the coupling moments and forces on the body exhibit comparatively significant errors. Validation errors for the body forces can be attributed in part to the fact that the total mass of the leg is not identifiable from fixed-base identification. Validation errors for the moments can be attributed in part to the fact that the rotational inertias of the first two rotors and links cannot be properly disambiguated without measuring the reaction moments on the body.

Although it is generally difficult to perform full floating-base identification, these results highlight the additional benefits that would be gained from including 6-axis force-torque (FT) measurements from a FT sensor attached to the base in the table-top experiments. These measurements would allow coupling forces on the body to be measured and additional parameters identified. This insight introduces an interesting scenario not considered in the current work. How is the structurally identifiable subspace influenced when FT sensing is available along axes other than the joint freedoms? Similarly, how is structural identifiability influenced when torque sensing is not available on some of the joints? The theoretical framework put forward in this paper presents a viable route to rigorously answer these and other further questions for parameter identifiability.

IX. CONCLUSIONS

This paper has introduced the recursive parameter nullspace algorithm (RPNA) to geometrically characterize the identifiability of inertial parameters in a rigid-body system. We have show that unidentifiable parameter combinations have an interpretation as representing a sequence of inertial transfers across the joints. In arriving at this result, we have transformed the nonlinear parameter observability problem for the system as a whole into a sequence of classical linear systems observability problems, proceeding recursively across each joint of the mechanism. As a result of these new theoretical advances, the final algorithm is compact (it can be expressed in under 10 lines), while generalizing the results of multiple previous authors. Extensions have been discussed to handle general multi-DoF joint models, branched kinematic trees, and simple closed loops arising from geared motors. The results verify the correctness of the algorithm and illustrate the importance of considering motion restrictions when designing identification strategies for mobile systems.

REFERENCES

[1] C. G. Atkeson, C. H. An, and J. M. Hollerbach, "Estimation of inertial parameters of manipulator loads and links," *The International Journal of Robotics Research*, vol. 5, no. 3, pp. 101–119, 1986.

[2] W. Khalil and F. Bennis, "Symbolic calculation of the base inertial parameters of closed-loop robots," *International Journal of Robotics Resesearch*, vol. 14, no. 2, pp. 112–128, 1995.

[3] J. Swevers, C. Ganseman, D. B. Tukel, J. de Schutter, and H. V. Brussel, "Optimal robot excitation and identification," *IEEE Transactions on Robotics and Automation*, vol. 13, no. 5, pp. 730–740, Oct 1997.

[4] K. Ayusawa, G. Venture, and Y. Nakamura, "Identification of the inertial parameters of a humanoid robot using unactuated dynamics of the base link," in *IEEE RAS Humanoids*, Dec 2008, pp. 1–7.

[5] ——, "Identification of flying humanoids and humans," in *2010 IEEE International Conference on Robotics and Automation*, May 2010, pp. 3715–3720.

[6] ——, "Identifiability and identification of inertial parameters using the underactuated base-link dynamics for legged multibody systems," *Int. J. of Robotics Research*, vol. 33, no. 3, pp. 446–468, 2014.

[7] S. Traversaro, A. D. Prete, R. Muradore, L. Natale, and F. Nori, "Inertial parameter identification including friction and motor dynamics," in *IEEE-RAS International Conference on Humanoid Robots (Humanoids)*, Oct 2013, pp. 68–73.

[8] J. Jovic, A. Escande, K. Ayusawa, E. Yoshida, A. Kheddar, and G. Venture, "Humanoid and human inertia parameter identification using hierarchical optimization," *IEEE Transactions on Robotics*, vol. 32, no. 3, pp. 726–735, June 2016.

[9] T. Lee, P. M. Wensing, and F. C. Park, "Geometric robot dynamic identification: A convex programming approach," *IEEE Transactions on Robotics*, vol. 36, no. 2, pp. 348–365, 2020.

[10] M. Gautier and W. Khalil, "Direct calculation of minimum set of inertial parameters of serial robots," *IEEE Transactions on Robotics and Automation*, vol. 6, no. 3, pp. 368–373, Jun 1990.

[11] H. Mayeda, K. Yoshida, and K. Osuka, "Base parameters of manipulator dynamic models," *IEEE Transactions on Robotics and Automation*, vol. 6, no. 3, pp. 312–321, Jun 1990.

[12] S.-Y. Sheu and M. W. Walker, "Identifying the independent inertial parameter space of robot manipulators," *The International journal of robotics research*, vol. 10, no. 6, pp. 668–683, 1991.

[13] H. Kawasaki, Y. Beniya, and K. Kanzaki, "Minimum dynamics parameters of tree structure robot models," in *International Conference on Industrial Electronics, Control and Instrumentation*, Oct 1991, pp. 1100–1105 vol.2.

[14] K. Chen, D. G. Beale, and D. Wang, "A new method to determine the base inertial parameters of planar mechanisms," *Mechanism and Machine Theory*, vol. 37, no. 9, pp. 971 – 984, 2002.

[15] J. Ros, X. Iriarte, and V. Mata, "3d inertia transfer concept and symbolic determination of the base inertial parameters," *Mechanism and Machine Theory*, vol. 49, pp. 284 – 297, 2012.

[16] R. Bellman and K. J. Aström, "On structural identifiability," *Mathematical Biosciences*, vol. 7, pp. 329–339, 1970.

[17] G. Calafiore and M. Indri, "Robust calibration and control of robotic manipulators," in *American Control Conf.*, 2000, pp. 2003–2007.

[18] N. Ramdani and P. Poignet, "Robust dynamic experimental identification of robots with set membership uncertainty," *IEEE/ASME Trans. on Mechatronics*, vol. 10, no. 2, pp. 253–256, April 2005.

[19] M. Gautier, "Numerical calculation of the base inertial parameters," *J Robotics Syst.*, vol. 8, pp. 485–506, 1991.

[20] P. K. Khosla, "Categorization of parameters in the dynamic robot model," *IEEE Transactions on Robotics and Automation*, vol. 5, no. 3, pp. 261–268, 1989.

[21] J. Ros, A. Plaza, X. Iriarte, and J. Aginaga, "Inertia transfer concept based general method for the determination of the base inertial parameters," *Multibody System Dynamics*, vol. 34, no. 4, pp. 327–347, Aug 2015.

[22] W. Khalil and J.-F. Kleinfinger, "Minimum operations and minimum parameters of the dynamic models of tree structure robots," *IEEE Journal on Robotics and Automation*, vol. 3, no. 6, pp. 517–526, 1987.

[23] J. Carpentier, G. Saurel, G. Buondonno, J. Mirabel, F. Lamiraux, O. Stasse, and N. Mansard, "The pinocchio c++ library: A fast and flexible implementation of rigid body dynamics algorithms and their analytical derivatives," in *2019 IEEE/SICE International Symposium on System Integration (SII)*. IEEE, 2019, pp. 614–619.

[24] C. D. Sousa and R. Cortesão, "Physical feasibility of robot base inertial parameter identification: A linear matrix inequality approach," *Int. J. of Robotics Research*, vol. 33, no. 6, pp. 931–944, 2014.

[25] P. M. Wensing, S. Kim, and J.-J. Slotine, "Linear matrix inequalities for phyiscally consistent inertial parameter identification: A statistical perspective on the mass distribution," *IEEE Robotics and Automation Letters*, 2017.

[26] T. Lee and F. C. Park, "Robust Dynamic Identification of Multibody Systems using Natural Distance Metric on Physically Consistent Inertial Parameters," *IEEE RAL*, no. 2, 2018.

[27] M. Gautier and W. Khalil, "Exciting trajectories for the identification of base inertial parameters of robots," *The International Journal of Robotics Research*, vol. 11, no. 4, pp. 362–375, 1992.

[28] G. Calafiore, M. Indri, and B. Bona, "Robot dynamic calibration: Optimal excitation trajectories and experimental parameter estimation," *Journal of robotic systems*, vol. 18, no. 2, pp. 55–68, 2001.

[29] J. Jovic, F. Philipp, A. Escande, K. Ayusawa, E. Yoshida, A. Kheddar, and G. Venture, "Identification of dynamics of humanoids: Systematic exciting motion generation," in *IEEE/RSJ Int. Conf. on Intelligent Rob. and Sys.*, Sept 2015, pp. 2173–2179.

[30] A. Janot, P. O. Vandanjon, and M. Gautier, "A generic instrumental variable approach for industrial robot identification," *IEEE Trans. on Control Systems Technology*, vol. 22, no. 1, pp. 132–145, Jan 2014.

[31] ——, "An instrumental variable approach for rigid industrial robots identification," *Control Engineering Practice*, vol. 25, pp. 85 – 101, 2014.

[32] A. Janot, P.-O. Vandanjon, and M. Gautier, "A revised durbin-wu-hausman test for industrial robot identification," *Control Engineering Practice*, vol. 48, pp. 52 – 62, 2016.

[33] G. Tournois, M. Focchi, A. D. Prete, R. Orsolino, D. Caldwell, and C. Semini, "Online payload identi cation for quadruped robots," in *IEEE/RSJ Int. Conf. on Intelligent Rob. and Sys.*, 2017.

[34] V. Bonnet, A. Crosnier, G. Venture, M. Gautier, and P. Fraisse, "Inertial parameters identification of a humanoid robot hanged to a fix force sensor," in *2018 IEEE International Conference on Robotics and Automation (ICRA)*, 2018, pp. 4927–4932.

[35] P. KHOSLA, "Real-time control and identification of direct-drive manipulators," *Ph. D. dissertation, Carnegie-Mellon Univ.*, 1986.

[36] W. Khalil, M. Gautier, and J. Kleinfinger, "Automatic generation of identification models of robots," *Int. J. of Robotics and Automation*, vol. 1, no. 1, pp. 2–6, 1986.

[37] G. D. Niemeyer, "Computational algorithms for adaptive robot control," Master's thesis, MIT, 1990.

[38] K. Chen and D. G. Beale, "A new symbolic method to determine base inertia parameters for general spatial mechanisms," in *International Design Engineering Technical Conferences and Computers and Information in Engineering Conference*, vol. 36223, 2002, pp. 731–735.

[39] X. Iriarte, J. Ros, F. Valero, V. Mata, and J. Aginaga, "Symbolic calculation of the base inertial parameters of a low mobility mechanism," in *Proc. ECCOMAS Multibody Dynamics*, 2013, pp. 1113–1124.

[40] R. Featherstone, *Rigid Body Dynamics Algorithms*. Springer, 2008.

[41] W. J. Rugh, *Linear Systems Theory*, 2nd ed. Prentice-Hall, Inc., 1996.

[42] R. Featherstone and D. Orin, "Chapter 2: Dynamics," in *Springer Handbook of Robotics*, B. Siciliano and O. Khatib, Eds. New York: Springer, 2008.

[43] J. Y. S. Luh, M. W. Walker, and R. P. C. Paul, "On-line computational scheme for mechanical manipulators," *ASME Journal of Dynamic Systems, Measurement, and Control*, vol. 102, no. 2, pp. 69–76, 1980.

[44] Z. Sun, S. Ge, and T. Lee, "Controllability and reachability criteria for switched linear systems," *Automatica*, vol. 38, no. 5, pp. 775 – 786, 2002.

[45] J. Craig, *Introduction to Robotics: Mechanics and Control*, 4th, Ed. Pearson, 2018.

[46] P. M. Wensing, A. Wang, S. Seok, D. Otten, J. Lang, and S. Kim, "Proprioceptive actuator design in the MIT Cheetah: Impact mitigation and high-bandwidth physical interaction for dynamic legged robots," *IEEE Transactions on Robotics*, vol. 33, no. 3, pp. 509–522, 2017.

APPENDIX A
RIGID-BODY DYNAMICS DETAILS

Spatial Velocities: The spatial velocity is a 6D velocity that collects traditional 3D rotational and linear velocities. When expressed in its body-fixed coordinate frame the spatial velocity of body i take the form

$$\mathbf{v}_i = \begin{bmatrix} \boldsymbol{\omega}_i \\ \boldsymbol{v}_i \end{bmatrix} \tag{45}$$

where $\boldsymbol{\omega}_i \in \mathbb{R}^3$ the angular velocity in body coordinates, and $\boldsymbol{v}_i \in \mathbb{R}^3$ the linear velocity of the coordinate origin (given in body coordinates).

Spatial Transform: The 6×6 matrix ${}^{i}\mathbf{X}_{i-1}$ is a spatial transformation matrix that converts spatial velocities expressed in frame i-1 to frame i:

$${}^{i}\mathbf{X}_{i\text{-}1} = \begin{bmatrix} {}^{i}\mathbf{R}_{i\text{-}1} & \mathbf{0} \\ -{}^{i}\mathbf{R}_{i\text{-}1}\,\mathbf{S}\left({}^{i\text{-}1}\mathbf{p}_i\right) & {}^{i}\mathbf{R}_{i\text{-}1} \end{bmatrix} \tag{46}$$

where ${}^{i}\mathbf{R}_{i-1} \in \mathbb{R}^3$ the rotation matrix from frame $i-1$ to frame i, ${}^{i\text{-}1}\mathbf{p}_i$ the vector from the origin of frame $i-1$ to the origin of frame i, and $\mathbf{S}(\mathbf{x}) \in \mathbb{R}^{3\times3}$ is the skew-symmetric 3D cross-product matrix satisfying $\mathbf{S}(\mathbf{x})\mathbf{y} = \mathbf{x}\times\mathbf{y}$ for all $\mathbf{x},\mathbf{y} \in \mathbb{R}^3$. Note that if ${}^{i}\mathbf{T}_{i\text{-}1}$ is the homogenous transform between frames i and i-1, then ${}^{i}\mathbf{X}_{i\text{-}1}$ is equivalent to the (big) Adjoint matrix $\mathrm{Ad}_{{}^{i}\mathbf{T}_{i\text{-}1}}$.

Spatial Cross Product: The 6×6 spatial cross product matrix is given by

$$\begin{bmatrix} \boldsymbol{\omega} \\ \boldsymbol{v} \end{bmatrix} \times = \begin{bmatrix} \mathbf{S}(\boldsymbol{\omega}) & 0 \\ \mathbf{S}(\boldsymbol{v}) & \mathbf{S}(\boldsymbol{\omega}) \end{bmatrix}$$

叉乘的运算方法

Similar to the standard 3D cross product, the spatial cross product can be used to provide the rate of change in a 6D quantity due to its expression in moving coordinates. Note that the 6×6 cross product matrix $(\mathbf{v}\times)$ is equivalent to the (little) adjoint matrix $\mathrm{ad}_{\mathbf{v}}$.

Spatial Inertia: The spatial Inertia $\mathbf{I}_i \in \mathbb{R}^6$ for body i is given using body-fixed coordinates by

$$\mathbf{I}_i = \begin{bmatrix} \bar{\mathbf{I}}_i & m_i\mathbf{S}(\mathbf{c}_i) \\ m_i\mathbf{S}(\mathbf{c}_i)^\top & m_i\mathbf{1}_3 \end{bmatrix}$$

with $\mathbf{c}_i \in \mathbb{R}^3$ the vector to the CoM of body i in local coordinates, $m_i \in \mathbb{R}_+$ its mass, and $\bar{\mathbf{I}}_i \in \mathbb{R}^{3\times3}$ a standard 3D rotational inertia tensor about the coordinate origin

$$\bar{\mathbf{I}}_i = \begin{bmatrix} I_{xx} & I_{xy} & I_{xz} \\ I_{xy} & I_{yy} & I_{yz} \\ I_{xz} & I_{yz} & I_{zz} \end{bmatrix}$$

APPENDIX B
SECOND EXAMPLE FOR FIXED-BASED SYSTEMS

For the system in Fig. 3(b), the velocity of body 2 and its span can be given by

$$\mathbf{v}_2 = \begin{bmatrix} \ell s_2 \dot{q}_1 \\ \ell c_2 \dot{q}_1 \\ \dot{q}_2 \\ 0 \\ 0 \\ -\ell \dot{q}_1 \end{bmatrix} \qquad \mathbf{V}_2 = \begin{bmatrix} 1 & 0 & 0 & 0 \\ 0 & 1 & 0 & 0 \\ 0 & 0 & 1 & 0 \\ 0 & 0 & 0 & 0 \\ 0 & 0 & 0 & 0 \\ 0 & 0 & 0 & 1 \end{bmatrix}$$

In comparison to the example system in Fig. 3(a), the span $\mathbf{V}_2$ has an extra column, representing additional motion freedoms for the second body of this non-planar system. This example also highlights that not all velocities in the span $\mathcal{V}_2$ are themselves attainable. It is observed that while the last column of $\mathbf{V}_2$ is in the span of attainable velocities, a pure linear velocity in the $\hat{z}_2$ direction is not possible.

The first body again only has a single identifiable parameter I_{zz_1}. Considering a transfer between body 1 and body 2, the momentum conditions $\mathbf{V}_2^\top \, \delta\mathbf{I}_2 \, \mathbf{\Phi}_2 = \mathbf{0}$ enforce

$$\delta I_{xz_2} = \delta I_{yz_2} = \delta I_{zz_2} = 0 \tag{47}$$

Similar to the previous case, these conditions impose that inertial changes to body 2 must not create angular momentum about $\hat{z}_2$. However, the change in joint geometries between the examples provides a different set of parameters that are identifiable via the second joint torque in this case.

The invariance conditions:

$$\mathbf{\Phi}_1^\top \, {}^2\mathbf{X}_1^\top(0) \, \delta\mathbf{I}_2^{(k)} \, {}^2\mathbf{X}_1(0) \, \mathbf{\Phi}_1 = 0$$

collectively enforce

$$\delta h_{x_2} = \delta h_{y_2} = \delta I_{xx_2} - \delta I_{yy_2} = \delta I_{xy_2} = 0 \tag{48}$$

for $k = 1, \ldots, 4$. The conditions are redundant for all larger k. Again, these conditions ensure that any variations how in $\delta\mathbf{I}_2$ maps to δI_{zz_1} must be zero. Note that the rotational inertia of Body 2 about $\hat{z}_1$ is

$$\begin{aligned} \mathbf{\Phi}_1^\top \, {}^2\mathbf{X}_1^\top \, \mathbf{I}_2 \, {}^2\mathbf{X}_1 \mathbf{\Phi}_1 = {} & m_2\ell^2 + c_2^2 I_{yy_2} + s_2^2 I_{xx_2} \\ & + 2c_2 s_2 I_{xy_2} + 2\ell c_2 h_{x_2} - 2\ell s_2 h_{y_2} \end{aligned}$$

This term staying constant with changes in q_2 is equivalent to (48), and can be deduced from conditions on its first four derivatives with respect to q_2.

APPENDIX C
INERTIA TRANSFERS: KINEMATIC CHAINS

Consider the change in kinetic energy:

$$\delta T = \frac{1}{2} \sum_{j=1}^{N} \mathbf{v}_j^\top \delta\mathbf{I}_j \mathbf{v}_j$$

Suppose a perturbation $\delta\boldsymbol{\pi}$ such that body i is the largest numbered body with $\delta\mathbf{I}_i \neq \mathbf{0}$. Then, using (**??**), the kinetic energy variation can be expressed as:

$$\begin{aligned} \delta T = {} & \frac{1}{2} \sum_{j=1}^{i-2} \left(\mathbf{v}_j^\top \delta\mathbf{I}_j \mathbf{v}_j \right) + \frac{1}{2} \mathbf{\Phi}_i^\top \delta\mathbf{I}_i \mathbf{\Phi}_i \dot{q}_i^2 \\ & + \mathbf{v}_{i\text{-}1}^\top \, {}^i\mathbf{X}_{i\text{-}1}^\top \delta\mathbf{I}_i \mathbf{\Phi}_i \dot{q}_i \\ & + \frac{1}{2} \mathbf{v}_{i\text{-}1}^\top \left[\delta\mathbf{I}_{i\text{-}1} + {}^i\mathbf{X}_{i\text{-}1}^\top \delta\mathbf{I}_i \, {}^i\mathbf{X}_{i\text{-}1} \right] \mathbf{v}_{i\text{-}1} \end{aligned} \tag{49}$$

Consider a linear change of variables for $\delta\mathbf{I}_{i\text{-}1}$:

$$\delta\mathbf{I}_{i\text{-}1} = \delta\mathbf{I}'_{i\text{-}1} - {}^i\mathbf{X}_{i\text{-}1}^\top(0) \delta\mathbf{I}_i \, {}^i\mathbf{X}_{i\text{-}1}(0) \tag{50}$$

which forms $\delta\mathbf{I}_{i\text{-}1}$ via an inertia transfer from the child plus an additional change $\delta\mathbf{I}'_{i\text{-}1}$. Under this change of variables (49) takes the decoupled form:

$$\delta T = \frac{1}{2} \sum_{j=1}^{i-2} \left(\mathbf{v}_j^\top \delta\mathbf{I}_j \mathbf{v}_j \right) + \frac{1}{2} \mathbf{v}_{i\text{-}1}^\top \delta\mathbf{I}'_{i\text{-}1} \mathbf{v}_{i\text{-}1} \tag{51}$$

$$+ \mathbf{v}_{i\text{-}1}^\top \, {}^i\mathbf{X}_{i\text{-}1}^\top \delta\mathbf{I}_i \mathbf{\Phi}_i \dot{q}_i + \frac{1}{2} \mathbf{\Phi}_i^\top \delta\mathbf{I}_i \mathbf{\Phi}_i \dot{q}_i^2 \tag{52}$$

$$+ \frac{1}{2} \mathbf{v}_{i\text{-}1}^\top \mathbf{\Delta}_i(q_i) \mathbf{v}_{i\text{-}1} \tag{53}$$

where $\mathbf{v}_{i-1} = {}^i\mathbf{X}_{i\text{-}1}(0)\mathbf{v}_{i\text{-}1}$ and $\mathbf{\Delta}_i$ is defined as

$$\mathbf{\Delta}_i(q_i) = \left({}^i\mathbf{X}_{J_i}^\top(q_i) \, \delta\mathbf{I}_i \, {}^i\mathbf{X}_{J_i}(q_i) - \delta\mathbf{I}_i \right)$$

For $\delta T = 0$ for all $\mathbf{q}, \dot{\mathbf{q}}$, the terms from (52) being zero is equivalent to

$$\mathbf{v}_i^\top \delta\mathbf{I}_i \mathbf{\Phi}_i = 0 \quad \forall \mathbf{q}, \dot{\mathbf{q}} \tag{54}$$

while the terms from (53) being zero is equivalent to

$$\mathbf{0} = \mathbf{v}_{i-1}^\top \, \mathbf{\Delta}_i(q_i) \, \mathbf{v}_{i-1} \quad \forall \mathbf{q}, \dot{\mathbf{q}} \tag{55}$$

Zeroing the remaining terms (51) is equivalent to $\delta T = 0$ for modifications, $\delta\mathbf{I}_1, \ldots, \delta\mathbf{I}_{i-2}$, $\delta\mathbf{I}'_{i-1}$ earlier in the chain.

APPENDIX D
ASIDE: REVISITING THE MAIN RESULT IN [6]

Ayusawa et al. provided a powerful result [6] that is summarized as follows. For a floating-base open-chain system, the inertial parameters that are identifiable through measurement of joint torques and external forces are the same as when joint torques are not available. This result has immediate application to identifying position-controlled robots. To relate these previous results with the approaches taken here, consider a partitioning of the equations of motion (1):

$$\begin{bmatrix} \mathbf{H}_1(\mathbf{q}) \\ \mathbf{H}_*(\mathbf{q}) \end{bmatrix} \ddot{\mathbf{q}} + \begin{bmatrix} \mathbf{c}_1(\mathbf{q}, \dot{\mathbf{q}}) + \mathbf{g}_1(\mathbf{q}) \\ \mathbf{c}_*(\mathbf{q}, \dot{\mathbf{q}}) + \mathbf{g}_*(\mathbf{q}) \end{bmatrix} = \begin{bmatrix} 0 \\ \boldsymbol{\tau}_J \end{bmatrix} + \begin{bmatrix} \mathbf{J}_1(\mathbf{q})^T \mathbf{f} \\ \mathbf{J}_*^\top \mathbf{f} \end{bmatrix} \tag{56}$$

where $\mathbf{H}_1$, $\mathbf{c}_1$, and $\mathbf{g}_1$ give the top rows of $\mathbf{H}$, $\mathbf{M}$, and $\mathbf{g}$ corresponding to the floating base, and $\mathbf{J}_1$ gives the left columns of $\mathbf{J}$ likewise corresponding to the floating base. The $*$ entries represent analogous entries for the joints, but won't be needed elsewhere in our development. The main result from [6] is re-phased below with an alternate proof that relies upon a short set of physical arguments.

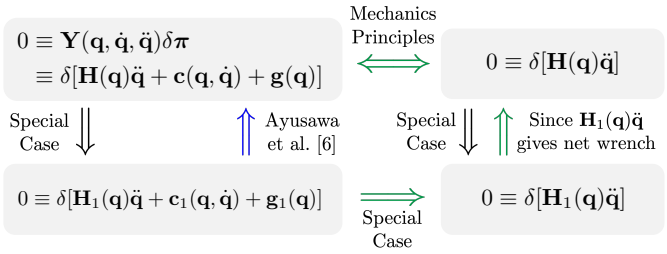

Fig. 10. An alternate proof of the main result from [6] uses mechanics principles. The implication from the blue arrow is replaced by those in green.

Theorem 3 (Main result of [6])**.** *Consider a floating-base open-chain rigid-body system with dynamics* (56)*. The parameter change $\delta\boldsymbol{\pi}$ doesn't effect the dynamics if and only if*

$$\delta[\mathbf{H}_1(\mathbf{q})\ddot{\mathbf{q}} + \mathbf{c}_1(\mathbf{q},\dot{\mathbf{q}}) + \mathbf{g}_1(\mathbf{q})] = \mathbf{0} \quad \forall \mathbf{q},\dot{\mathbf{q}},\ddot{\mathbf{q}} \tag{57}$$

Proof. ($\Rightarrow$) The forward implication is immediate since the conditions in (57) are a subset of those required for $\delta\boldsymbol{\pi} \in \mathcal{N}$.

($\Leftarrow$) Toward proving the reverse implication, we first consider a number of equivalences. Per Remark 2, we can ignore gravity, so $\delta\boldsymbol{\pi}$ leaves the dynamics unchanged if and only if:

$$\delta[\mathbf{H}(\mathbf{q})\ddot{\mathbf{q}} + \mathbf{c}(\mathbf{q},\dot{\mathbf{q}})] = \mathbf{0} \quad \forall \mathbf{q},\dot{\mathbf{q}},\ddot{\mathbf{q}}$$

Since the Coriolis terms are determined uniquely from the form of the mass matrix (e.g., via Christoffel symbols), this condition is equivalent to requiring that

$$\delta[\mathbf{H}(\mathbf{q})\ddot{\mathbf{q}}] = \mathbf{0} \quad \forall \mathbf{q},\ddot{\mathbf{q}} \tag{58}$$

The condition (58) is also equivalent to enforcing that $\delta\mathbf{H}(\mathbf{q}) \equiv 0$ as was considered in the previous subsection.

Let us consider the case when only joint j is moving. In that case, we have from (30) that $\mathbf{H}_1\ddot{\mathbf{q}} = {}^{j}\mathbf{X}_1^{\top}\mathbf{I}_j^{C}\boldsymbol{\Phi}_j\ddot{q}_j$, which represents the total wrench required to move all bodies in the system. By comparison, consider the joint torque at any joint i earlier in the chain ($i < j$), given by

$$\tau_i = H_{ij}\ddot{q}_j = \boldsymbol{\Phi}_i^{\top\,j}\mathbf{X}_i^{\top}\mathbf{I}_j^{C\,j}\mathbf{X}_1^{\top}\boldsymbol{\Phi}_j\ddot{q}_j = \boldsymbol{\Phi}_i^{\top\,1}\mathbf{X}_i^{\top}\mathbf{H}_1\ddot{\mathbf{q}}$$

In this case, τ_i is simply the projection of the net wrench onto the i-th joint. As such, the i-th joint torque carries strictly less information than $\mathbf{H}_1\ddot{\mathbf{q}}$. By this logic, if

$$\delta[\mathbf{H}_1(\mathbf{q})\ddot{\mathbf{q}}] = \mathbf{0} \quad \forall \mathbf{q},\ddot{\mathbf{q}} \tag{59}$$

then the upper-triangle of $\delta\mathbf{H}(\mathbf{q})$ will be zero for all $\mathbf{q}$. Via symmetry of $\mathbf{H}$, this implies that $\delta\mathbf{H}(\mathbf{q}) = 0$ for all $\mathbf{q}$.

Zooming out, we have argued that $\delta\boldsymbol{\pi}$ doesn't affect the dynamics if and only if (59) holds. Since condition (57) implies (59), our proof of the reverse implication is complete. □

We hope that this conceptual, but physically grounded proof will help enhance the appeal of the original main result in [6] for a broader range of readers.

Appendix E
Proof of Lemma 1

To prove the lemma in the main text, we begin with a proposition to compute the span of velocities that can be reached after a joint given a span of velocities before it.

Proposition 1. *Consider a spatial transform as a function of a single angle q, denoted $\mathbf{X}(q)$. Suppose $\mathbf{X}(0) = \mathbf{1}$ and further that*

$$\frac{\partial \mathbf{X}(q)}{\partial q} = -\boldsymbol{\Phi} \times \mathbf{X}(q) \tag{60}$$

for some $\boldsymbol{\Phi} \in \mathbb{R}^{6\times 1}$. Then, for any $\mathbf{V} \in \mathbb{R}^{6\times k}$

$$\begin{aligned} &\operatorname{span}\{\mathbf{v} \mid \exists q \in \mathbb{R}, \mathbf{v} \in \operatorname{Range}(\mathbf{X}(q)\,\mathbf{V})\} \\ &\quad = \operatorname{Range}(\operatorname{Ctrb}((\boldsymbol{\Phi}\times), \mathbf{V})) \end{aligned} \tag{61}$$

where $\operatorname{Ctrb}((\boldsymbol{\Phi}\times), \mathbf{V}))$ gives the controllability matrix associated with the pair $((\boldsymbol{\Phi}\times), \mathbf{V}))$ [41].

Proof of Proposition 1. We define

$$\mathcal{S}(\boldsymbol{\Phi}, \mathbf{V}) = \operatorname{span}\{\mathbf{X}(q)\mathbf{v} \mid \mathbf{v} \in \operatorname{Range}(\mathbf{V})\}$$

and recall, from the Lemma statement, that

$$\frac{\mathrm{d}}{\mathrm{d}q}\mathbf{X}(q) = -(\boldsymbol{\Phi}\times)\mathbf{X}(q)$$

From the definition of the matrix exponential for a linear system [41]:

$$\mathbf{X}(q)\mathbf{V} = \mathrm{e}^{-q(\boldsymbol{\Phi}\times)}\mathbf{V}$$

The Cayley-Hamilton theorem then ensures that

$$\mathcal{S}(\boldsymbol{\Phi}, \mathbf{V}) \subseteq \operatorname{Range}\left([\mathbf{V}, (\boldsymbol{\Phi}\times)\mathbf{V}, \ldots, (\boldsymbol{\Phi}\times)^5\mathbf{V}]\right)$$

and thus

$$\mathcal{S}(\boldsymbol{\Phi}, \mathbf{V}) \subseteq \operatorname{Range}(\operatorname{Ctrb}((\boldsymbol{\Phi}\times), \mathbf{V}))$$

Note, the range of the controllability matrix provides the smallest $(\boldsymbol{\Phi}\times)$-invariant subspace containing $\operatorname{Range}(\mathbf{V})$. Yet, $\mathcal{S}(\boldsymbol{\Phi}, \mathbf{V})$ is invariant under $(\boldsymbol{\Phi}\times)$ and contains $\operatorname{Range}(\mathbf{V})$. This proves the reverse containment. □

Proof of Lemma 1. The propagation of the attainable velocity span:

$$\mathbf{V}_i = \left[\operatorname{Ctrb}\left((\boldsymbol{\Phi}_i\times), {}^{i}\mathbf{X}_{i\text{-}1}(0)\,\mathbf{V}_{i\text{-}1}\right)\ \boldsymbol{\Phi}_i\right]$$

follows from Proposition 1 and Eq. (**??**).

□

Appendix F
Proof of Lemma 2

The following proposition is key to proving Lemma 2.

Proposition 2. *Consider a spatial transform as a function of a single angle q, denoted $\mathbf{X}(q)$. Suppose $\mathbf{X}(0) = \mathbf{1}$ and consider $\boldsymbol{\Phi} \in \mathbb{R}^{6\times 1}$ such that*

$$\frac{\partial \mathbf{X}(q)}{\partial q} = -\boldsymbol{\Phi} \times \mathbf{X}(q)$$

For any $\mathbf{C} \in \mathbb{R}^{k\times 10}$, the following holds

$$\begin{aligned} &\{\boldsymbol{\pi} \in \mathbb{R}^{10} \mid \mathbf{C}\left[\mathbf{X}^{\top}(q)\,[\boldsymbol{\pi}]^{\wedge}\,\mathbf{X}(q)\right]^{\vee} = 0,\ \forall q \in \mathbb{R}\} \\ &=\operatorname{Null}(\operatorname{Obs}(\mathbf{C}, \mathbf{A}(\boldsymbol{\Phi}))) \end{aligned}$$

where $\operatorname{Obs}(\mathbf{C}, \mathbf{A}(\boldsymbol{\Phi}))$ is the observability matrix [41] associated with the pair $(\mathbf{C}, \mathbf{A}(\boldsymbol{\Phi}))$.

Either set in the equality characterizes the inertial parameters that maintain a zero output with respect to $\mathbf{C}$ following transformation across a joint with free modes $\mathbf{\Phi}$.

Proof of Proposition 2. Let $\boldsymbol{\pi}_0 \in \mathbb{R}^{10}$ and denote

$$\boldsymbol{\pi}(q) = [\, \mathbf{X}^\top(q)\, [\boldsymbol{\pi}_0]^\wedge\, \mathbf{X}(q)\,]^\vee$$

Using (**??**), (34), and the fact that $\mathbf{X}(q)$ and $(\mathbf{\Phi}\times)$ commute:

$$\begin{aligned}\frac{\mathrm{d}}{\mathrm{d}q}\boldsymbol{\pi}(q) &= -\left[\, (\mathbf{\Phi}\times)^\top\, [\boldsymbol{\pi}(q)]^\wedge + [\boldsymbol{\pi}(q)]^\wedge\, (\mathbf{\Phi}\times)\,\right]^\vee \\ &= -\mathbf{A}(\mathbf{\Phi})\, \boldsymbol{\pi}(q)\end{aligned}$$

Linear systems observability results [41] then guarantee that the following are equivalent

$$\begin{aligned}&\boldsymbol{\pi}_0 \in \mathrm{Null}\,(\,\mathrm{Obs}\,(\,\mathbf{C},\, \mathbf{A}(\mathbf{\Phi})\,)\,) \\ \iff\quad &\boldsymbol{\pi}(q) \in \mathrm{Null}(\mathbf{C}) \quad \forall q\end{aligned}$$

□

Proof of Lemma 2. Suppose $\delta\mathbf{I}_i$ such that

$$\mathbf{v}_i^\top \delta\mathbf{I}_i \mathbf{v}_i = 0 \quad \forall \mathbf{q}, \dot{\mathbf{q}}$$

This is equivalent to

$$\left[{}^i\mathbf{X}_{i-1}\mathbf{v}_{i-1} + \mathbf{\Phi}_i\dot{q}_i\right]^\top \delta\mathbf{I}_i \left[{}^i\mathbf{X}_{i-1}\mathbf{v}_{i-1} + \mathbf{\Phi}_i\dot{q}_i\right] = 0$$

for all $\mathbf{q}, \dot{\mathbf{q}}$. Expanding terms, this implies

$$\begin{aligned}0 &= \mathbf{v}_{i-1}^\top {}^i\mathbf{X}_{i\text{-}1}^\top(0) {}^i\mathbf{X}_{J_i}^\top(q_i) \delta\mathbf{I}_i {}^i\mathbf{X}_{J_i}(q_i) {}^i\mathbf{X}_{i\text{-}1}(0)\mathbf{v}_{i-1} \quad \forall \mathbf{q}, \dot{\mathbf{q}} \\ 0 &= \mathbf{\Phi}_i^\top \delta\mathbf{I}_i \mathbf{v}_i \quad \forall \mathbf{q}, \dot{\mathbf{q}}\end{aligned}$$

with the first condition equivalent to

$$\mathbf{0} = \mathbf{K}_{i-1}\, {}^{i\text{-}1}\mathbf{B}_{i^-} \left[{}^i\mathbf{X}_{J_i}^\top(q_i) \delta\mathbf{I}_i {}^i\mathbf{X}_{J_i}(q_i)\right]^\vee \quad \forall q_i$$

and the second equivalent to

$$\mathbf{M}(\mathbf{V}_i, \mathbf{\Phi}_i)\, \delta\boldsymbol{\pi}_i = \mathbf{0}$$

where $\mathbf{M}(\mathbf{V}_i, \mathbf{\Phi}_i)$ is given by (32). Using Proposition 2, it follows that $\mathbf{K}_i$ can be selected as

$$\mathbf{K}_i = \begin{bmatrix} \mathrm{Obs}(\, \mathbf{K}_{i-1}\, {}^{i\text{-}1}\mathbf{B}_{i^-},\, \mathbf{A}(\mathbf{\Phi}_i)\,) \\ \mathbf{M}(\mathbf{V}_i, \mathbf{\Phi}_i) \end{bmatrix}$$

□

Appendix G
Identifiability from Gravity

Similar to the nullspace for the kinetic energy, variations ensuring $\delta\mathbf{g} = 0$ can be formed via sequences of inertia transfers. The variation $\delta\mathbf{g}$ to the generalized gravitational force is equal to zero if and only if the rate of change in potential energy $\delta\dot{V} = 0$. This is given by:

$$\delta\dot{V} = -\dot{\mathbf{q}}^\top \mathbf{g} = \sum_{j=1}^{N} \mathbf{v}_j^\top\, \delta\mathbf{I}_j\, {}^j\mathbf{X}_0\, {}^0\mathbf{a}_g$$

Each entry of the sum characterizes a change in the instantaneous power of the gravitational force on Body j. We again assume that body i is the largest body with $\delta\mathbf{I}_i \neq \mathbf{0}$, and follow a similar approach to the kinetic energy nullspace analysis. Following an equivalent derivation to Appendix C it can be shown that $\delta\mathbf{g} = \mathbf{0}$ iff

$$\mathbf{0} = {}^0\mathbf{a}_g^\top\, {}^i\mathbf{X}_0^\top\, \delta\mathbf{I}_i\, \mathbf{\Phi}_i \tag{62}$$

$$0 = \mathbf{v}_{i-1}^\top\, \mathbf{\Delta}_i(q_i)\, {}^{J_i}\mathbf{X}_0\, {}^0\mathbf{a}_g \tag{63}$$

for all $\mathbf{q}, \dot{\mathbf{q}}$, and subsequent changes $\delta\mathbf{I}_1, \ldots, \delta\mathbf{I}_{i-2}, \delta\mathbf{I}'_{i\text{-}1}$ independently satisfy $\delta\mathbf{g} = \mathbf{0}$. Similar to before, the substitution introducing $\delta\mathbf{I}'_{i\text{-}1}$ via (50) decouples considerations of transfers across joint i from transfers earlier in the chain.

Condition (62) motivates the attainable gravity vector span

$$\mathcal{A}_i = \mathrm{span}\left\{{}^i\mathbf{X}_0(\mathbf{q})\, {}^0\mathbf{a}_g \mid \mathbf{q} \in \mathbb{R}^N\right\}$$

Analogous to Lemma 1, we seed $\mathbf{A}_0 = {}^0\mathbf{a}_g$ and recursively apply

$$\mathbf{A}_i = \mathrm{Ctrb}(\, (\mathbf{\Phi}_i\times), {}^i\mathbf{X}_{i\text{-}1}(0)\, \mathbf{A}_{i\text{-}1}\,)$$

which ensures each $\mathrm{Range}(\mathbf{A}_i) = \mathcal{A}_i$. Intuitively, changes satisfying $\mathbf{A}_i^\top \delta\mathbf{I}_i \mathbf{\Phi}_i = \mathbf{0}$ cannot be detected via the preceding joint torque in static cases.

The second condition (63) can be addressed by generalizing the propagation of $\mathbf{K}_i$ from Lemma 2 to include gravitational effects. This extension can be accomplished by including the new parameters that are identified via static torques on each joint:

$$\mathbf{K}_i = \begin{bmatrix} \mathrm{Obs}(\, \mathbf{K}_{i-1}\, {}^{i\text{-}1}\mathbf{B}_{i^-},\, \mathbf{A}(\mathbf{\Phi}_i)\,) \\ \mathbf{M}([\mathbf{V}_i\, \mathbf{A}_i], \mathbf{\Phi}_i) \end{bmatrix}$$

Comparing the propagation of $\mathbf{A}_i$ and $\mathbf{V}_i$

$$\mathbf{V}_0 = \mathbf{0} \qquad \mathbf{V}_i = [\, \mathrm{Ctrb}(\, (\mathbf{\Phi}_i\times), \mathbf{V}_{i^-}\,)\ \ \mathbf{\Phi}_i\,] \tag{64}$$

$$\mathbf{A}_0 = {}^0\mathbf{a}_g \qquad \mathbf{A}_i = \mathrm{Ctrb}(\, (\mathbf{\Phi}_i\times), {}^i\mathbf{X}_{i\text{-}1}(0)\, \mathbf{A}_{i\text{-}1}\,) \tag{65}$$

a union of these bases $\tilde{\mathbf{V}}_i = [\mathbf{V}_i,\, \mathbf{A}_i]$ can be propagated together in one operation via:

$$\tilde{\mathbf{V}}_0 = {}^0\mathbf{a}_g \quad \tilde{\mathbf{V}}_i = \left[\, \mathrm{Ctrb}\Big(\, (\mathbf{\Phi}_i\times), {}^i\mathbf{X}_{i\text{-}1}(0)\tilde{\mathbf{V}}_{i-1}\Big)\ \ \mathbf{\Phi}_i\,\right] \tag{66}$$

which simply represents a change in seed for $\mathbf{V}_0$.

Appendix H
Computing the System Parameter Nullspace

For each body, consider $\mathbf{R}_i$ as any full rank matrix such that $\mathrm{Range}(\mathbf{R}_i) = \mathrm{Null}(\mathbf{N}_i)$. With this local nullspace basis, we construct a block upper-triangular matrix $\mathbf{R}$ such that

$$\begin{aligned}\mathbf{R}_{i,i} &= \mathbf{R}_i \\ \mathbf{R}_{i\text{-}1,i} &= -{}^{i\text{-}1}\mathbf{B}_{i^-}\, \mathbf{R}_i \quad \text{when } i\text{-}1 > 0\end{aligned}$$

and $\mathbf{R}_{i,j} = \mathbf{0}$ otherwise. Following this construction $\mathrm{Range}(\mathbf{R}) = \mathcal{N}$. Similarly, we can use the local nullspace descriptors $\mathbf{N}_i$ to determine a basis for $\mathcal{N}^\perp$. A system nullspace descriptor $\mathbf{N}$ is constructed as an upper-triangular block matrix satisfying

$$\begin{aligned}\mathbf{N}_{i,i} &= \mathbf{N}_i \\ \mathbf{N}_{i,j} &= \mathbf{N}_{i,j\text{-}1}\, {}^{j\text{-}1}\mathbf{B}_{j^-} \quad \forall j < i\end{aligned}$$

and $\mathbf{N}_{i,j} = \mathbf{0}$ otherwise. Following this construction, $\mathrm{Null}(\mathbf{N}) = \mathcal{N}$ and thus, $\mathrm{Range}(\mathbf{N}^\top) = \mathcal{N}^\perp$. The signifi-

cance of this property is that each row of $\mathbf{N}$ describes a linear combination of parameters that can be identified. The row-reduced-echelon form of $\mathbf{N}$ allows identifiable parameters (individually or through regroupings) to be plainly discerned.